

The Development of MPI Modelling in PYTHIA*

Torbjörn Sjöstrand

*Theoretical Particle Physics, Department of Astronomy and Theoretical Physics,
Lund University, SE-223 62 Lund, Sweden*

Abstract

Many of the basic ideas in multiparton interaction (MPI) phenomenology were first developed in the context of the PYTHIA event generator, and MPIs have been central in its modelling of both minimum-bias and underlying-event physics in one unified framework. This chapter traces the evolution towards an increasingly sophisticated description of MPIs in PYTHIA, including topics such as the ordering of MPIs, the regularization of the divergent QCD cross section, the impact-parameter picture, colour reconnection, multiparton PDFs and beam remnants, interleaved and intertwined evolution, and diffraction.

*To be published in "Multiple Parton Interactions at the LHC", P. Bartalini and J. R. Gaunt, eds., World Scientific

1 Introduction

The PYTHIA event generator [1] was initially created to explore the physics of colour flow in hadronic collisions, in analogy with how the Lund string model [2] had successfully predicted string effects in e^+e^- annihilation [3, 4]. Initially only $2 \rightarrow 2$ partonic (q, g, γ) processes were implemented, with colour flow connecting the scattered partons to the beam remnants, followed by string fragmentation using JETSET [5]. At the 1984 Snowmass workshop on the SSC, when I first got directly involved in the physics of high-energy hadron colliders, it was obvious that this approach was too primitive to be of relevance. During the autumn I implemented initial- and final-state radiation (ISR and FSR) [6], with the expectation that this further activity would give event topologies more comparable with $Spp\bar{p}S$ data. In terms of jet phenomenology it did, but underlying events were still much less active than in data.

The natural explanation, in my opinion, was that the composite nature of the proton would lead to several parton–parton interactions, giving more activity. Thus in the spring of 1985 I developed a first multiparton interaction (MPI) model, still primitive but offering a significantly improved description of data, convincing me that MPIs was the way to go. Not everybody approved; the first writeup [7] was not accepted for publication. In 1986 studies resumed, and several further key aspects were introduced [8]. In its basic ideology this formalism has remained, even if the details have been improved and extended many times over the years.

This evolution will be described in the following, and in the process an overview will be given of all the components of the current framework. While PYTHIA-centered, external sources of inspiration (in a positive or negative sense) will be mentioned, with emphasis on the early days, when the basic ideas were formulated. Much more information can be obtained from the companion articles of this book, about other models and generators, and about all the experimental studies that have been undertaken over the years. Notably, no experimental plots are shown, since relevant ones are already reproduced elsewhere, see [9–16], often compared with PYTHIA and other generators.

2 Early data and models

In the eighties, the $Spp\bar{p}S$ was providing new data on hadronic collisions, at an order of magnitude higher CM energy than previously available, from 200 to 900 GeV. It came to change our understanding of hadronic collisions. Some observations are of special interest for the following.

- The width $\sigma(n_{\text{ch}})$ of the charged multiplicity distribution is increasing with energy such that $\sigma(n_{\text{ch}})/\langle n_{\text{ch}} \rangle$ stays roughly constant [17, 18], “KNO scaling” [19], actually even slowly getting broader. A close-to Poissonian process, in longitudinal phase space or in the fragmentation of a single straight string, instead would predict a $1/\sqrt{\langle n_{\text{ch}} \rangle}$ narrowing.
- Multiplicity fluctuations show long-range “forward–backward” correlations [20], defined by

$$b_{\text{FB}}(\Delta\eta) = \frac{\langle n_{\text{F}} n_{\text{B}} \rangle - \langle n_{\text{F}} \rangle^2}{\langle n_{\text{F}}^2 \rangle - \langle n_{\text{F}} \rangle^2}, \quad (1)$$

where n_F and n_B is the (charged) multiplicity in two symmetrically located unit-width pseudorapidity bins, separated by a central variable-width $\Delta\eta$ gap. Again this is not expected in Poissonian processes.

- The average transverse momentum $\langle p_\perp \rangle$ increases with increasing charged multiplicity [21, 22]. This is opposite to the behaviour at lower energies, where energy-momentum conservation effects dominate, with a crossover at the highest ISR energies [23].
- A non-negligible fraction of the total cross section is associated with minijet production [24, 25], increasing from $\sim 5\%$ at 200 GeV to $\sim 15\%$ at 900 GeV. Here UA1 defined a minijet as a region $\Delta R = \sqrt{(\Delta\eta)^2 + (\Delta\varphi)^2} \leq 1$ with $\sum E_\perp > 5$ GeV.
- The increase of the total $p\bar{p}$ cross section $\sigma_{\text{tot}}(s)$ rather well matches that of the minijet one $\sigma_{\text{minijet}}(s)$, *i.e.* $\sigma_{\text{tot}}(s) - \sigma_{\text{minijet}}(s)$ is almost constant [24, 25].
- Events with a minijet have a rather flat $\langle p_\perp \rangle(n_{\text{ch}})$, while ones without show a strong rise, starting from a lower level [24].
- The fraction of events having several minijets is non-negligible. (Rates up to 5 are quoted from workshop presentations in Ref. [8], but apparently never published.)
- Events containing a hard jet also have an above-average level of particle production well away from the jet core [26], the “pedestal effect”. Of note is that the pedestal increases rapidly up to $E_{\perp\text{jet}} \sim 10$ GeV, and then flattens out, even dropping slightly [25].
- Also the jet profiles are affected by this extra source of activity.
- By contrast, there were no early studies on double parton scattering (DPS) at the $Spp\bar{p}S$. The first observation instead came from AFS at ISR [27], in a study of pairwise balancing jets in four-jet events, but it did not convince everybody.

On the theoretical side, the basic idea of MPI existed [28–34], see also [35]. These first studies almost exclusively considered DPS, without a vision of an arbitrary number of scatterings. Studies often only included scattering of valence quarks, since the large- x region was needed to access “large” jet p_\perp scales. Therefore DPS/MPI was only expected to correspond to a tiny fraction of the total cross section. If needed, a $p_{\perp\text{min}}$ cutoff would be introduced at a sufficiently high value to make it so.

For soft physics, the Pomeron language was predominant, notably in its Dual Topological Unitarization (DTU) formulation, both to describe total cross sections and event topologies [36–47]. In it a cut Pomeron corresponds to two multiperipheral chains, or strings in Lund language, stretched directly between the two beam remnants after the collision. In most of the earlier phenomenological studies only one cut Pomeron was used, but extensions to multiple Pomerons were introduced for $Spp\bar{p}S$ applications. Then the number of cut Pomerons can vary freely, *e.g.* according to a Poissonian. Uncut Pomerons, *i.e.* virtual corrections, ensure unitarity. This approach was quite successful in describing aspects of the data such as the charged multiplicity distribution and forward–backward correlations.

In contrast to the unitarization approach, the good match between the rise of $\sigma_{\text{tot}}(s)$ and $\sigma_{\text{minijet}}(s)$ led to speculations that $\sigma_{\text{tot}}(s)$ (or at least its inelastic component) could be written as an incoherent sum $\sigma_{\text{tot}}(s) = \sigma_{\text{soft}} + \sigma_{\text{minijet}}(s)$ [48–50].

At the time, there appears to have been little “middle ground” between the hard MPI, the soft multi-Pomeron and the UA1-minijet ways of approaching physics.

On the generator side, ISAJET [51] was state of the art. It described one hard interaction with its showers, and then added an underlying event (UE) based on the Pomeron approach.

The UE was intended to reproduce minimum-bias (MB) event properties at the hard-interaction-reduced collision energy. Since it was based on independent fragmentation the two components could be easily decoupled. Other generators for hard interactions [52, 53] had more primitive UE descriptions, and the one generator for MB [54] did not include hard interactions. In addition (unpublished) longitudinal phase-space models tuned to inclusive data were used within the experimental collaborations, ultimately refined into the UA5 generator [55].

3 The first PYTHIA model

Against this backdrop, the key new idea of the first PYTHIA model [7] was to reinterpret the multi-Pomeron picture in terms of multiple perturbative QCD interactions. Thus there would no longer be the need for separate descriptions of MB and UE physics. A hard-process event would just be the high- p_{\perp} tail of the MB class, and a soft-process event just one where the hardest jet was too soft to detect as such. MPIs come out as an unavoidable consequence, not only as a tiny tail of hard DPS events, but as representing the bulk of the inelastic nondiffractive cross section σ_{nd} at higher energies.

By contrast, no importance could be attached to the 5 GeV UA1 minijet cutoff scale or to the seemingly simple relationship between $\sigma_{\text{tot}}(s)$ and $\sigma_{\text{minijet}}(s)$ that it led to. On the contrary, MPIs had to extend much lower in p_{\perp} in order to give enough varying activity to describe *e.g.* the approximate KNO scaling. Here jet universality was assumed, *i.e.* that the underlying fragmentation mechanism was the same string as described e^+e^- data so well, only applied to a more complicated partonic state.

In its technical implementation, the starting point of the model is the differential perturbative QCD $2 \rightarrow 2$ cross section

$$\frac{d\sigma}{dp_{\perp}^2} = \sum_{i,j,k} \iiint f_i(x_1, Q^2) f_j(x_2, Q^2) \frac{d\hat{\sigma}_{ij}^k}{d\hat{t}} \delta\left(p_{\perp}^2 - \frac{\hat{t}\hat{u}}{\hat{s}}\right) dx_1 dx_2 d\hat{t}, \quad (2)$$

with $Q^2 = p_{\perp}^2$ as factorization and renormalization scale. The corresponding integrated cross section depends on the chosen $p_{\perp\text{min}}$ scale:

$$\sigma_{\text{int}}(p_{\perp\text{min}}) = \int_{p_{\perp\text{min}}^2}^{s/4} \frac{d\sigma}{dp_{\perp}^2} dp_{\perp}^2, \quad (3)$$

see Fig. 1.

Diffractive events presumably give a small fraction of the perturbative jet activity, and elastic none, so the simple model sets out to describe only inelastic nondiffractive events, with an approximately known σ_{nd} . It is thus concluded that the average such event ought to contain

$$\langle n_{\text{MPI}}(p_{\perp\text{min}}) \rangle = \frac{\sigma_{\text{int}}(p_{\perp\text{min}})}{\sigma_{\text{nd}}} \quad (4)$$

hard interactions. An average above unity corresponds to more than one such subcollision per event, which is allowed by the multiparton structure of the incoming hadrons. If the interactions were to occur independently of each other, $n_{\text{MPI}}(p_{\perp\text{min}})$ would be distributed

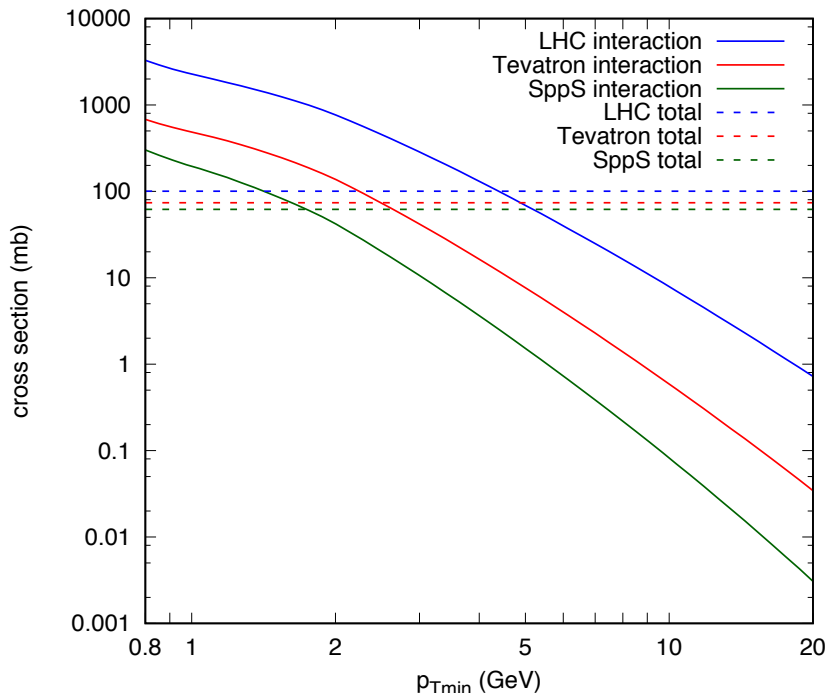


Figure 1: The integrated interaction cross section $\sigma_{\text{int}}(p_{\perp\text{min}})$ for the $Spp\bar{p}S$ at 630 GeV, Tevatron at 1.96 TeV and LHC at 13 TeV. For comparison the total cross section σ_{tot} at the respective energy is indicated by a horizontal line, with the nondiffractive part σ_{nd} at order 60% of this. Results have been obtained with the PYTHIA 8.223 default values, including the NNPDF2.3 QCD+QED LO PDF set with $\alpha_s(M_Z) = 0.130$ [56].

according to a Poissonian. But such an approach would be flawed, *e.g.* sometimes using up more energy for collisions than is available.

The solution to this problem was inspired by the parton-shower paradigm. The generation of consecutive MPIs is formulated as an evolution downwards in p_{\perp} , resulting in a sequence of n interactions with $\sqrt{s}/2 > p_{\perp 1} > p_{\perp 2} > \dots > p_{\perp n} > p_{\perp\text{min}}$. The probability distribution for $p_{\perp 1}$ becomes

$$\frac{d\mathcal{P}}{dp_{\perp 1}} = \frac{1}{\sigma_{\text{nd}}} \frac{d\sigma}{dp_{\perp 1}} \exp\left(-\int_{p_{\perp 1}}^{\sqrt{s}/2} \frac{1}{\sigma_{\text{nd}}} \frac{d\sigma}{dp'_{\perp}} dp'_{\perp}\right). \quad (5)$$

Here the naive probability is corrected by an exponential factor expressing that there must not be any interaction in the range between $\sqrt{s}/2$ and $p_{\perp 1}$ for $p_{\perp 1}$ to be the hardest interaction. The procedure can be iterated, to give

$$\frac{d\mathcal{P}}{dp_{\perp i}} = \frac{1}{\sigma_{\text{nd}}} \frac{d\sigma}{dp_{\perp i}} \exp\left(-\int_{p_{\perp i}}^{p_{\perp i-1}} \frac{1}{\sigma_{\text{nd}}} \frac{d\sigma}{dp'_{\perp}} dp'_{\perp}\right). \quad (6)$$

The exponential factors resemble Sudakov form factors of parton showers [57, 58], or uncut Pomerons for that matter, and fills the same function of ensuring probabilities bounded by unity. Summing up the probability for a scattering at a given p_{\perp} scale to happen at any step of the generation chain gives back $(1/\sigma_{\text{nd}}) d\sigma/dp_{\perp}$, and the number of interactions

above any p_{\perp} is a Poissonian with an average of $\sigma_{\text{int}}(p_{\perp})/\sigma_{\text{nd}}$, as it should. The downwards evolution in p_{\perp} is routinely handled by using the veto algorithm [59], like for showers.

The similarities with showers should not be overemphasized, however. While the shower p_{\perp} scale has some approximate relationship to an evolution in time, this is not so for MPIs. Rather, when the two Lorentz-contracted hadron “pancakes” collide, the MPIs can be viewed as occurring simultaneously in different parts of the overlap region. What is instead gained is a way to handle the parton distribution functions (PDFs) of several partons in the same hadron, at the very least to conserve overall energy and momentum. Specifically, it is for the hardest MPI that conventional PDFs have been tuned and tested, so we had better respect that. For subsequent MPIs no PDF data exist, so some adjustments are acceptable. In this first implementation only rescaled PDFs

$$f(x'_i, Q^2) \quad \text{with} \quad x'_i = \frac{x_i}{1 - \sum_{j=1}^{i-1} x_j} < 1 \quad (7)$$

are used for the i 'th interaction. This rescaling suppresses the tail towards events with many MPIs, so the n_{MPI} distribution becomes narrower than Poissonian.

To complement the model, a number of further details of the simulation had to be specified, often intended as temporary solution.

- There is a finite probability that no MPIs at all are generated above $p_{\perp\text{min}}$. For this set of events, small but not negligible, an infinitely soft gluon exchange is assumed, leading to two strings stretched directly between the beam remnants.
- Only the hardest interaction is allowed to be any combination of incoming and outgoing flavours, weighted according to Eq. (2). For subsequent ones kinematics is chosen the same way, with modified PDFs, but afterwards the process is always set up to be of the $gg \rightarrow gg$ type. The reason is to avoid complicated beam-remnant structures.
- The colour flow of the hardest interaction is described by the original PYTHIA algorithm [1]. Two extreme scenarios for the colour flow of the non-hardest MPIs were compared. In the simplest one, each such gives rise to a double string stretched between the two outgoing gluons of the MPI, disconnected from the rest of the event.
- By the choices above, where only the hardest interaction affects the flavour and colour of the beam remnant, a limited number of remnant types can be obtained. If a valence quark is kicked out, a diquark is left behind. If a gluon, the leftover colour octet state of a proton can be split into a quark and a diquark that attach to two separate strings. If the two remnants then share the longitudinal momentum evenly, it maximizes the particle production. This gives too few low-multiplicity events, and also leaves less room for MPIs to build up a high-multiplicity tail, assuming that the average is kept fixed. Therefore a probability distribution is used wherein the quark often obtains much less momentum than the diquark. Finally, if a sea (anti)quark is kicked out, the remnant can be split into a single hadron plus a quark or diquark.
- Only the hardest interaction is dressed up with showers, whereas the subsequent ones are not. Again the reason is beam-remnant issues, but one excuse is that most non-hardest MPIs appear at low p_{\perp} scales, where little further radiation should be allowed.

The key free parameter of this framework is $p_{\perp\text{min}}$. The lower it is chosen, the higher the average number of MPIs, cf. Eq. (3), and thus the higher the average charged multiplicity $\langle n_{\text{ch}} \rangle$. To agree with 540 GeV UA5 data [17] a value of $p_{\perp\text{min}} = 1.6$ GeV was required.

The dependence of $\langle n_{\text{ch}} \rangle$ on $p_{\perp\text{min}}$ is quite strong so, if everything else is kept fixed, the $p_{\perp\text{min}}$ uncertainty is of order ± 0.1 GeV. The most agreeable aspect, however, is that with $p_{\perp\text{min}}$ tuned, the shape of the n_{ch} distribution is reasonably well described. Without MPIs the shape is Poissonian-like, also when a single hard interaction is allowed. With MPIs instead an approximate KNO scaling behaviour is obtained, driven by the n_{MPI} distribution. (Which, even if also a Poissonian, obeys $\langle n_{\text{MPI}} \rangle \ll \langle n_{\text{ch}} \rangle$, meaning much larger relative fluctuations $\sigma/\langle n \rangle$.) By the same mechanism also strong forward–backward correlations are obtained, where before these were tiny. That is, the n_{MPI} is a kind of global quantum number of an event, that affects whether particle production is high or low over the whole rapidity range. With some damping, since not all strings are stretched equally far out to the beam remnants.

In part this is nothing new; the number of cut Pomerons in soft models fills a similar function for both n_{MPI} distributions and forward–backward correlations. What is new is that an application of perturbation theory, in combination with string fragmentation, can give a reasonable description also of minimum-bias physics. This unifies hard and soft physics at colliders, as being part of the same framework. It also introduces a new cutoff scale in QCD, with a value different from other scales, such as the proton mass.

It was clear from the onset that the model was incomplete in its details, and the listed open questions for the model well matches the problems that have later been studied.

- What is the correct behaviour of $d\sigma/dp_{\perp}^2$ at small p_{\perp} ? A sharp cutoff, below which cross sections vanish, is not plausible.
- How to remove (or, if not, interpret) the class of events with no MPIs, currently represented by a $p_{\perp} = 0$ interaction?
- How to introduce an impact-parameter picture, giving more activity for central collisions and less for peripheral? This is needed to give an a bit wider n_{ch} distribution. Also, for UA1 jets the MPI formalism as it stands at this stage only gives about a quarter of the observed pedestal effect.
- How to achieve a better description of multiparton PDFs, that also consistently includes *e.g.* flavour conservation and correlations?
- Where does the baryon number go if several valence quarks are kicked out from a proton?
- How does the colour singlet nature of the incoming beams translate into colour correlations between the different MPIs?
- What is the structure and role of beam remnants?
- By confinement and the uncertainty relation the incoming partons must have some random nonperturbative transverse motion. How should such “primordial k_{\perp} ” effects be included? These then have to be compensated in the remnants, and furthermore the remnant parts may have relative k_{\perp} values of their own.
- How should parton-shower effects be combined consistently between the systems? The flavour, colour and beam-remnant issues reappear here.
- How important is ISR evolution wherein a parton branches into two that participate in two separate interactions?
- How important is rescattering, *i.e.* when one parton can scatter consecutively from two or more partons from the other hadron?
- How do diffractive topologies contribute to the picture? Typical experimental “min-

imum bias” triggers catch a fraction of these events, which have different properties from the nondiffractive ones. The low-multiplicity end of the n_{ch} distribution was left unexplained in the studies, with the motivation that it is dominated by diffraction.

- How do the results scale with collision energy? With a fixed $p_{\perp\text{min}}$ scale it was possible to reproduce the $\langle n_{\text{ch}} \rangle$ evolution from fixed-target to 900 GeV, and this was the basis for extrapolations.

4 Smooth damping and impact-parameter dependence

For the first published MPI article [8], the original framework was extended to address some of the most pressing shortcomings above. (The older approach was also retained as a simpler alternative. Unfortunately the new approach led to longer computer generation times, which was a real issue at the time.)

The sharp cutoff $p_{\perp\text{min}}$ is replaced by a smooth turnoff at a scale $p_{\perp 0}$. To be specific, the cross section of Eq. (2) is multiplied by a damping factor

$$\left(\frac{\alpha_s(p_{\perp 0}^2 + p_{\perp}^2)}{\alpha_s(p_{\perp}^2)} \frac{p_{\perp}^2}{p_{\perp 0}^2 + p_{\perp}^2} \right)^2. \quad (8)$$

Since the QCD $2 \rightarrow 2$ processes are dominated by t -channel gluon exchange, which behaves like $1/\hat{t}^2 \sim 1/p_{\perp}^4$, this means that

$$\frac{d\sigma}{dp_{\perp}^2} \sim \frac{\alpha_s^2(p_{\perp}^2)}{p_{\perp}^4} \rightarrow \frac{\alpha_s^2(p_{\perp 0}^2 + p_{\perp}^2)}{(p_{\perp 0}^2 + p_{\perp}^2)^2}, \quad (9)$$

which is finite in the limit $p_{\perp} \rightarrow 0$. This behaviour can be viewed as a consequence of colour screening: in the $p_{\perp} \rightarrow 0$ limit a hypothetical exchanged gluon would not resolve individual partons but only (attempt to) couple to the vanishing net colour charge of the hadron. Technically the damping factor is multiplying the $d\hat{\sigma}/d\hat{t}$ expressions, but it could equally well have been imposed (half each) on the PDFs instead, since neither can be trusted for $p_{\perp} \rightarrow 0$.

In this modified framework all interactions are associated with a $p_{\perp} > 0$ scale, and at least one interaction must occur when two hadrons pass by for there to be an event at all. Thus we require $\sigma_{\text{int}}(0) > \sigma_{\text{nd}}$, where the σ_{int} integration, Eq. (3), now includes the damping factor. A tune to $\langle n_{\text{ch}} \rangle$ at 540 GeV gives $p_{\perp 0} \approx 2.0$ GeV, *i.e.* of the same order as the sharp $p_{\perp\text{min}}$ cutoff. The two would have been even closer, had not factorization and renormalization scales here been multiplied by 0.075, as suggested at the time to obtain an approximate NLO jet cross section [60]. Below $S\bar{p}\bar{p}S$ energies a fixed $p_{\perp 0}$ gives too small a $\sigma_{\text{int}}(0)$, so in this form the model is primarily intended for high-energy collider physics.

The other main change was to introduce a dependence on the impact parameter b of the collision process. To do this, a spherically symmetric matter distribution $\rho(\mathbf{x}) d^3x = \rho(r) d^3x$ is assumed. In a collision process the overlap of the two hadrons is then given by

$$\begin{aligned} \tilde{\mathcal{O}}(b) &= \iint d^3x dt \rho_{\text{boosted}} \left(x - \frac{b}{2}, y, z - vt \right) \rho_{\text{boosted}} \left(x + \frac{b}{2}, y, z + vt \right) \\ &\propto \iint d^3x dt \rho(x, y, z) \rho(x, y, z - \sqrt{b^2 + t^2}), \end{aligned} \quad (10)$$

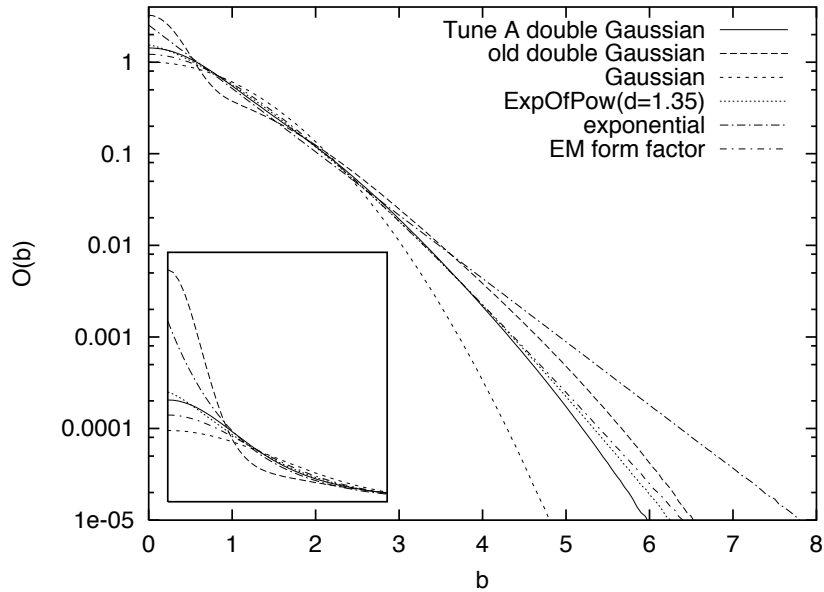


Figure 2: Examples of impact-parameter profiles $\tilde{\mathcal{O}}(b)$, some introduced only later. Somewhat arbitrarily the different parametrizations have been normalized to the same area and average b , *i.e.* same $\int \tilde{\mathcal{O}}(b) d^2b$ and $\int b\tilde{\mathcal{O}}(b) d^2b$. Insert shows the region $b < 2$ on a linear scale. From Ref. [61].

where the second line is obtained by suitable scale changes.

A few different ρ distributions were studied, Fig. 2. Using Gaussians is especially convenient, since the convolution then becomes trivial. A simple Gaussian was the starting point, but we found it did not give a good enough description of the data. Instead the preferred choice was a double Gaussian

$$\rho(r) = (1 - \beta) \frac{1}{a_1^3} \exp\left(-\frac{r^2}{a_1^2}\right) + \beta \frac{1}{a_2^3} \exp\left(-\frac{r^2}{a_2^2}\right). \quad (11)$$

This corresponds to a distribution with a small core region, of radius a_2 and containing a fraction β of the total hadronic matter, embedded in a larger hadron of radius a_1 . The choice of a not-so-smooth shape was largely inspired by the “hot spot” ideas popular at the time [62, 63]. The starting point is that, as a consequence of parton cascading, partons may tend to cluster in a few small regions, typically associated with the three valence quarks.

More convoluted ansätze could have been considered, but having two free parameters, β and a_2/a_1 , was sufficient to give the necessary flexibility.

It is now assumed that the interaction rate, to first approximation, is proportional to the overlap

$$\langle \tilde{n}_{\text{MPI}}(b) \rangle = k \tilde{\mathcal{O}}(b). \quad (12)$$

For each given b the number of interactions is assumed distributed according to a Poissonian, at least before energy–momentum conservation issues are considered. Zero interactions means that the hadrons pass each other without interacting. The $\tilde{n}_{\text{MPI}}(b) \geq 1$ interaction probability therefore is

$$\mathcal{P}_{\text{int}}(b) = 1 - \exp(-\langle \tilde{n}_{\text{MPI}}(b) \rangle) = 1 - \exp(-k \tilde{\mathcal{O}}(b)). \quad (13)$$

We notice that $k\tilde{\mathcal{O}}(b)$ is essentially the same as the eikonal $\Omega(s, b) = 2\text{Im}\chi(s, b)$ of optical models [64–67], but split into one piece $\tilde{\mathcal{O}}(b)$ that is purely geometrical and one $k = k(s)$ that carries the information on the parton–parton interaction cross section. Furthermore, this is (so far) only a model for nondiffractive events, so does not attempt to relate the eikonal to total or diffractive cross sections.

Simple algebra shows that the average number of interactions in events, *i.e.* hadronic passes with $n_{\text{MPI}} \geq 1$, is given by

$$\langle n \rangle = \frac{\int k \tilde{\mathcal{O}}(b) d^2b}{\int \mathcal{P}_{\text{int}}(b) d^2b} = \frac{\sigma_{\text{int}}(0)}{\sigma_{\text{nd}}}, \quad (14)$$

which fixes the absolute value of k (numerically).

For event generation, Eq. (5) generalizes to

$$\frac{d\mathcal{P}}{d^2b dp_{\perp 1}} = \frac{\tilde{\mathcal{O}}(b)}{\langle \tilde{\mathcal{O}} \rangle} \frac{1}{\sigma_{\text{nd}}} \frac{d\sigma}{dp_{\perp 1}} \exp\left(-\frac{\tilde{\mathcal{O}}(b)}{\langle \tilde{\mathcal{O}} \rangle} \int_{p_{\perp 1}}^{\sqrt{s}/2} \frac{1}{\sigma_{\text{nd}}} \frac{d\sigma}{dp'_{\perp}} dp'_{\perp}\right), \quad (15)$$

with the definition

$$\langle \tilde{\mathcal{O}} \rangle = \frac{\int \tilde{\mathcal{O}}(b) d^2b}{\int \mathcal{P}_{\text{int}}(b) d^2b}. \quad (16)$$

Hence $\tilde{\mathcal{O}}(b)/\langle \tilde{\mathcal{O}} \rangle$ represents the enhancement at small b and depletion at large b . The simultaneous selection of $p_{\perp 1}$ and b is somewhat more tricky. In practice different schemes are used, depending on context.

- For minimum-bias events Eq. (15) can be integrated over $p_{\perp 1}$ to give $\mathcal{P}_{\text{int}}(b)$ of Eq. (13). To pick such a b it is useful to note that $\mathcal{P}_{\text{int}}(b) < \min(1, k\tilde{\mathcal{O}}(b))$ and split the b range accordingly. Once b is fixed the selection of $p_{\perp 1}$ can be done as for Eq. (5), only with an extra fix $\tilde{\mathcal{O}}(b)/\langle \tilde{\mathcal{O}} \rangle$, both in the prefactor and in the exponential. If $p_{\perp 1} = 0$ is reached in the downwards evolution without an interaction having been found, which happens with probability $\exp(-k\tilde{\mathcal{O}}(b))$, then the generation is restarted at the maximum scale $\sqrt{s}/2$.
- For a very hard process the exponential of Eq. (15) is very close to unity and can be dropped. Then the selection of b and $p_{\perp 1}$ decouples and can be done separately. Here $d\sigma/dp_{\perp 1}$ can represent any hard process, not only QCD jets, and $p_{\perp 1}$ any set of relevant kinematic variables.
- For a medium-hard process one can begin as in the hard case, and then use the exponential as an acceptance probability. If the hard-process kinematics is considered fixed then only a new b value is chosen in case of rejection. Note that it is always the QCD cross section that enters in the exponential. (Or, to be proper, the sum of all possible reactions, but that is completely dominated by QCD.) For non-QCD processes the $p_{\perp 1}$ scale in the exponential has to be associated with some suitable hardness scale, like the mass for the production of a resonance.

Once the hardest interaction is chosen, the generation of subsequent ones proceeds by a logical extension of Eq. (6) to

$$\frac{d\mathcal{P}}{dp_{\perp i}} = \frac{\tilde{\mathcal{O}}(b)}{\langle \tilde{\mathcal{O}} \rangle} \frac{1}{\sigma_{\text{nd}}} \frac{d\sigma}{dp_{\perp i}} \exp\left(-\frac{\tilde{\mathcal{O}}(b)}{\langle \tilde{\mathcal{O}} \rangle} \int_{p_{\perp i}}^{p_{\perp i-1}} \frac{1}{\sigma_{\text{nd}}} \frac{d\sigma}{dp'_{\perp}} dp'_{\perp}\right). \quad (17)$$

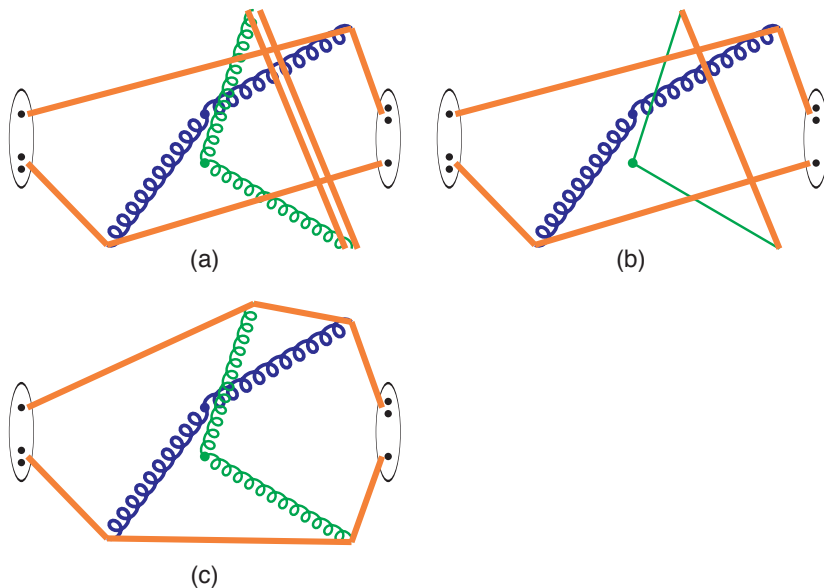


Figure 3: Colour drawing possibilities in the final state for the simple model. Thick blue gluons denote outgoing partons from the primary interaction, thin green gluons or quark lines the partons of a further MPI, black ovals the beam remnants with valence quarks, and orange thick lines the colour strings stretched between the partons. While the primary interaction and its connection to the beam remnants is handled according to the colour flow of the matrix elements, in the $N_C \rightarrow \infty$ limit [68], the further MPIs give a mix of behaviours (a), (b) and (c), as described in the text. Note that the figure is not to scale; *e.g.* that the strings have a transverse width of hadronic size.

There is one subtlety to note about ordering, however. QCD interactions have to be ordered in p_\perp for the formalism to reproduce the correct inclusive cross section. This applies for the MB generation, which gives an arbitrary $p_{\perp 1}$, and also in a sample of hard jets above some large $p_{\perp \min}$ scale. But it does not hold for non-QCD hard processes. For Z^0 production, say, which is not part of the normal MPI machinery, the second MPI (counting the Z^0 as the first) can go all the way up to the kinematic limit in p_\perp without involving any double-counting, with p_\perp -ordering only kicking in for the third MPI.

With MPIs stretching down to $p_\perp = 0$, the need arises to evaluate PDFs below their lower limit Q_0 scale, typically 1 – 2 GeV. To first approximation this is done by freezing them below Q_0 , but some attempts were made to enhance the relative importance of valence quarks for $Q \rightarrow 0$, since this is what one should expect to happen.

As before, colour drawing for all MPIs except the hardest one is handled in a primitive manner. Given that the kinematics of an interaction has been chosen with the full cross section, the final state is picked among three possibilities, Fig. 3, by default with equal probability.

- (a) Assume the collision to have produced a gg pair and stretch two string pieces directly between them, giving a closed gluon loop.
- (b) Assume the collision to have produced a $q\bar{q}$ pair and stretch a string directly between them.
- (c) Assume the collision to have produced a gg pair, but insert them separately on an

already existing string in such a way so as to minimize the increase of string length λ [69]. Here

$$\lambda \approx \sum_{i=0}^n \ln \left(1 + \frac{m_{i,i+1}^2}{m_0^2} \right), \quad m_{i,i+1}^2 = (\epsilon_i p_i + \epsilon_{i+1} p_{i+1})^2, \quad (18)$$

for a string $q_0 g_1 g_2 \cdots g_n \bar{q}_{n+1}$, where $\epsilon_q = 1$ but $\epsilon_g = 1/2$ because a gluon momentum is shared between two string pieces it is connected to.

Neither of these three follow naturally from any colour flow rules, such as t -channel gluon exchange. Rather the first two represent the simplest way to decouple different interaction systems from each other, not having to trace colours back through the beam remnants. If MPIs are such separated systems, and thus on the average each gives the same $\langle p_\perp \rangle$, then an essentially flat $\langle p_\perp \rangle(n_{\text{ch}})$ would be expected, since the study of the n_{ch} distribution tells us that higher n_{ch} values is a consequence of more MPIs rather than of harder jets. To obtain a rising $\langle p_\perp \rangle(n_{\text{ch}})$ it is therefore essential to have a mechanism to connect the different MPI subsystems in colour, not only at random but specifically so as to reduce the total string length of the event, more and more the more MPIs there are. Each further MPI on the average then contributes less n_{ch} than the previous, while still the same (semi)hard p_\perp kick is to be shared between the hadrons, thus inducing the rising trend. This is precisely what the third and last component is intended to do. It is the first large-scale application of colour reconnection (CR) ideas, previous applications having been for more specific channels such as $B \rightarrow J/\psi$ decays [70–72].

A very simple model for diffraction was also added, wherein the diffractive mass M is selected according to dM^2/M^2 and is represented by a single string stretched between a diquark in the forward direction and a quark in the backward one.

With these changes to the original model it is possible to obtain a quite reasonable description of essentially all the key experimental data outlined in Sec. 2. Above all, the model offered physics explanations for the behaviour observed in data.

- For the charged multiplicity distribution, improvements in the high-multiplicity tail originate from the introduction of an impact-parameter picture, whereas the addition of diffraction improves the low-multiplicity one. To describe the energy dependence, where $\sigma(n_{\text{ch}})/\langle n_{\text{ch}} \rangle$ is slightly increasing with energy, the impact-parameter dependence is crucial, since the $\sigma(n_{\text{MPI}})/\langle n_{\text{MPI}} \rangle$ then does not fall, which it otherwise would when $\langle n_{\text{MPI}} \rangle$ increases with energy. Also forward-backward correlations now are even stronger, reflecting the broader n_{MPI} distribution, and actually even somewhat above data. A number of other minimum-bias distributions look fine, like the $dn_{\text{ch}}/d\eta$ spectrum, inclusively as well as split into multiplicity bins, except for the lowest one, which is dominated by diffraction.
- The $\langle p_\perp \rangle(n_{\text{ch}})$ distribution is well described, both inclusively and split into samples with our without minijets. As already mentioned, the new CR mechanism here plays a key role to get the correct rising trend in the inclusive case, and to counteract the drop otherwise expected in the jet sample. Not only the slope but also the absolute value of $\langle p_\perp \rangle$ is well reproduced, without any need to modify the fragmentation p_\perp width tuned to e^+e^- data. This is one of the key observations that lend credence to the jet universality concept.
- The UA1 minijet studies are rather well reproduced. Notably the default double

Gaussian is needed to obtain the observed fraction with several minijets. The simpler alternatives with a single Gaussian, no b dependence, or no MPIs at all fared increasingly worse, even with α_s tuned to give the same average number of minijets.

- The pedestal effect, *i.e.* how the underlying event activity first rises with the trigger jet/cluster E_\perp , is well described, and explained. The rise is caused by a shift in the composition of events, from one dominated by fairly peripheral collisions to one strongly biased towards central ones. In the model there is a limit for how far this biasing can go: the exponential in Eq. (15)) can be neglected once $p_{\perp 1} \simeq E_\perp$ is so large that $\sigma_{\text{int}}(p_{\perp 1}) \ll \sigma_{\text{nd}}$. This happens at around 10 GeV, explaining the origin of that scale. The probability distribution is then given by $\tilde{\mathcal{O}}(b) d^2b$ independently of the $p_{\perp 1}$ value. The double Gaussian is required to obtain the correct pedestal height, whereas a single Gaussian undershoots. A slight drop of the pedestal height for $E_\perp > 25$ GeV can be attributed to a shift from mainly gg interactions to mainly $q\bar{q}$ ones.

In summary, most if not all of MB and UE physics at collider energies is explained and reasonably well described once the basic MPI framework has been complemented by a smooth turnoff of the cross section for $p_\perp \rightarrow 0$, a requirement to have at least one MPI to get an event, an impact-parameter dependence, and a colour reconnection mechanism.

5 Interlude

While the $Spp\bar{p}S$ had paved the way for a new view on hadronic collisions, the Tevatron rather contributed to cement this picture. KNO distributions kept on getting broader [73], forward-backward correlations got stronger [74], and $\langle p_\perp \rangle (n_{\text{ch}})$ showed the same rising trend [75, 76], to give some examples. The Tevatron emphasis was on hard physics, however, and it took many years to go beyond the $Spp\bar{p}S$ MB and UE studies. Notable is the CDF study on the production of $\gamma + 3$ jets [77], which came to be the first generally accepted proof of the existence of DPS. Studies of the pedestal effect eventually also became quite sophisticated [78–81], providing differential information on activity in towards, away and transverse regions in azimuth relative to the trigger, including a Z^0 trigger. All of these observations were in qualitative agreement with PYTHIA predictions. An improved quantitative agreement was obtained in a succession of tunes [82, 83], see also [9], like the much-used Tune A.

Even if agreement may not have been perfect, there was no obvious pattern of disagreement between $Spp\bar{p}S$ /Tevatron data and the PYTHIA model. Therefore it could routinely be used for experimental studies and for extrapolations to LHC and SSC energies. But it also meant that further MPI development was slow in the period 1988 – 2003, with only some relevant points, as follows.

More up-to-date formulae for total, elastic and diffractive cross sections were implemented [84], starting from the $\sigma_{\text{tot}}(s)$ parametrizations of Donnachie and Landshoff (DL) [85]. They are based on an effective Pomeron description, with parameters adjusted to describe existing data and also give a reasonable extrapolation to high energies. They worked well through the Tevatron era, but overestimated the diffractive rate for LHC and have since been modified.

The $p_{\perp 0}$ parameter went through several iterations, as new PDF sets appeared on the

market and became defaults in PYTHIA. Notably HERA data showed that there is a non-negligible rise in the small- x region, even for small Q^2 scales, whereas pre-HERA PDFs had tended to enforce a flat $xf(x, Q_0^2)$ at small x . This implies that the all- p_\perp integrated QCD cross section rises much faster with s than assumed before, and thereby generates a faster rising $\langle n_{\text{ch}} \rangle(s)$. The need for an s dependence of $p_{\perp 0}$, which previously had been marginal, now became obvious. Initially a logarithmic s dependence was used. Later on a power-like form was introduced, such as

$$p_{\perp 0}(s) = (2.1 \text{ GeV}) \left(\frac{s}{1 \text{ TeV}^2} \right)^\epsilon \quad (19)$$

with $\epsilon = 0.08$, inspired by the DL ansatz $\sigma_{\text{tot}}(s) \simeq s^\epsilon$, which also qualitatively matches well with a HERA $xf(x, Q_0^2) \simeq x^{-\epsilon}$ behaviour.

In an attempt to understand the behaviour of $p_{\perp 0}(s)$, a simple toy study was performed [86]. As we already argued, the origin of a $p_{\perp 0}$ damping scale in the first place is that the proton is a colour singlet, which means that individual parton colour charges are screened. A very naive estimate is that the screening distance should be the inverse of the proton size, $p_{\perp 0} \approx \hbar/r_p \approx 0.3 \text{ fm}$. But this assumes that the proton only consists of very few partons, such that the typical distance between two partons is r_p . In reality we expect the evolution of PDFs, especially at small x , to lead to a much higher density. Therefore the typical colour screening distance — how far away you need to go to find partons with opposing colour charges — to be much smaller than r_p . In order to test this, we built a model for the transverse structure of the proton as follows. Start out from a picture with three valence quarks and two “valence gluons” that share the full momentum of the proton at a scale $Q_0 \approx 0.5 \text{ GeV}$, based on the GRV PDF approach [87], distributed across a transverse proton disc, and with net vanishing colour. They are then evolved upwards in Q^2 , to create ISR cascades. A technical problem is that the $x \rightarrow 0$ singularity would generate infinitely many partons. Therefore branchings are only allowed if both daughters have an $x > x_{\text{min}} \simeq p_{\perp 0}/\sqrt{s}$. Colours are preserved in branchings, and daughters can drift a random amount in transverse space of order \hbar/Q if produced at a scale Q . A damping factor can then be defined by

$$\frac{|\sum_k q_k e^{i\mathbf{r}_k \mathbf{p}_\perp}|^2}{\sum_k |q_k|^2}, \quad (20)$$

where \mathbf{p}_\perp represents a gluon plane wave probing the proton, consisting of partons with colour charge q_k located at \mathbf{r}_k . This approach indeed gives results consistent with a damping at scales around 2 GeV, varying with s about as outlined above, but it contains too many uncertainties to be used for any absolute predictions.

The MPI framework was extended to γp [88] and $\gamma\gamma$ [89] collisions. It there was applied to the Vector Meson Dominance (VMD) part of the photon wave function, where the γ fluctuates into a virtual meson, predominantly a ρ^0 . The same framework as for $pp/p\bar{p}$ collisions can then be recycled, with modest modifications.

To finish this section, a few words on theory and on MPI modelling in some other Tevatron-era (and beyond) generators.

Generally, MPI ideas were gradually becoming more accepted. An interesting (partial) alternative was raised by the CCFM equations [90, 91], which interpolate between the DGLAP [92–94] and BFKL [95, 96] ones. Already BFKL allows p_\perp -unordered evolution chains, and with CCFM such a behaviour can be extended to higher p_\perp scales. As illustrated

in the LDC model [97], this can then give what looks like several (semi)hard interactions within one single chain.

ISAJET remained in use, even if slowly losing ground, with an essentially unchanged description of the underlying event.

When HERWIG was extended to hadronic collisions [98], it used an UE model/parametrization based on the UA5 MB generator [55], which is purely soft physics. MPIs were never made part of the Fortran HERWIG core code. Instead the UA5-based default could be replaced by the separate JIMMY [99] add-on. Its basic ideas resemble the ones in PYTHIA, but with several significant differences. The impact-parameter profile is given by the electromagnetic form factor, and at each given b the number of MPIs (in addition to the hard process itself) is given by a Poissonian with an average proportional to the convolution of two form factors. These MPIs are unordered in p_{\perp} , and all use unmodified PDFs. Instead interactions that break energy-momentum conservation are rejected. To handle beam remnants, it is assumed that each ISR shower initiator, except the first, is a gluon; if not an additional ISR branching is made to ensure this. Thereby it is possible to chain each MPI to the next in colour, such that the remnant flavour structure is related only to the first interaction. This handling allows all MPIs to be associated with ISR and FSR, unlike PYTHIA at the time. Note that JIMMY was intended for UE studies, and that HERWIG+JIMMY did not offer an MB option. Such a framework was developed [100] but the code for it was never made public. Only with the C++ version [101] did MPIs become a fully integrated part of the core code, for UE and MB [102, 103].

Another (later) multipurpose generator entrant is SHERPA [104], which so far has based itself on the PYTHIA MPI framework, but a new separate MPI model is under development [105].

Many generators geared towards minimum-bias physics also adapted semihard MPI ideas. Notably, generators based on eikonalization procedures typically already had contributions for soft and diffractive MPI-style physics, and could add a further contribution for hard MPIs. This means that a nondiffractive event can contain variable numbers of soft $p_{\perp} = 0$ and hard $p_{\perp} > p_{\perp\text{min}}$ MPIs. Typically a Gaussian b dependence is used, not necessarily with the same width for all contributions. Main examples of such programs are DTUJET [106,107], PHOJET [108,109], DPMJET [110], SIBYLL [111,112], EPOS [113,114], see also [115], and QGSJET [116,117]. It would carry too far to go into the details of these programs. Some of them are in use at the LHC, and describe minimum-bias data quite successfully. They are not only used for pp collisions but often also for pA and AA , and for cosmic-ray cascades in the atmosphere.

6 Multiparton PDFs and beam remnants

In 2004 the PYTHIA MPI model was significantly upgraded [61], specifically to allow a more realistic description of multiparton PDFs and beam remnants. Then ISR and FSR could also be included for each MPI, not only the hardest one.

To extend the PDF framework, it is assumed that quark distributions can be split into one valence and one sea part. In cases where this is not explicit in the PDF parametrizations, it is assumed that the sea is flavour-antiflavour symmetric, so that one can write *e.g.*

$$u(x, Q^2) = u_{\text{val}}(x, Q^2) + u_{\text{sea}}(x, Q^2) = u_{\text{val}}(x, Q^2) + \bar{u}(x, Q^2). \quad (21)$$

The parametrized $u(x, Q^2)$ and $\bar{u}(x, Q^2)$ distributions can then be used to find the relative probability for a kicked-out u quark to be either valence or sea.

For valence quarks two effects should be considered. One is the reduction in content by previous MPIs: if a u valence quark has been kicked out of a proton then only one remains, and if two then none remain. In addition the constraint from momentum conservation should be included, as already introduced in Eq. (7). Together this gives

$$u_{i,\text{val}}(x, Q^2) = \frac{N_{u,\text{val},\text{remain}}}{N_{u,\text{val},\text{original}}} \frac{1}{X} u_{\text{val}}\left(\frac{x}{X}, Q^2\right) \quad \text{with} \quad X = 1 - \sum_{j=1}^{i-1} x_j, \quad (22)$$

for the u quark in the i 'th MPI, and similarly for the d . The $1/X$ prefactor ensures that the u_i integrates to the remaining number of valence quarks. The momentum sum is also preserved, except for the downwards rescaling for each kicked-out valence quark. The latter is compensated by an appropriate scaling up of the gluon and sea PDFs.

When a sea quark (or antiquark) q_{sea} is kicked out of a hadron, it must leave behind a corresponding antisea parton in the beam remnant, by flavour conservation, which can then participate in another interaction. We can call this a companion antiquark, \bar{q}_{cmp} . In the perturbative approximation the pair comes from a gluon branching $g \rightarrow q_{\text{sea}} + \bar{q}_{\text{cmp}}$. This branching often would not be in the perturbative regime, but we choose to make a perturbative ansatz, and also to neglect subsequent perturbative evolution of the q_{cmp} distribution. Even if approximate, this procedure should catch the key feature that a sea quark and its companion should not be expected too far apart in x (or, better, in $\ln x$). Given a selected x_{sea} , the distribution in $x = x_{\text{cmp}} = y - x_{\text{sea}}$ then is

$$\begin{aligned} q_{\text{cmp}}(x; x_{\text{sea}}) &= C \int_0^1 g(y) P_{g \rightarrow q_{\text{sea}} \bar{q}_{\text{cmp}}}(z) \delta(x_{\text{sea}} - zy) dz \\ &= C \frac{g(x_{\text{sea}} + x)}{x_{\text{sea}} + x} P_{g \rightarrow q_{\text{sea}} \bar{q}_{\text{cmp}}}\left(\frac{x_{\text{sea}}}{x_{\text{sea}} + x}\right). \end{aligned} \quad (23)$$

Here $P_{g \rightarrow q\bar{q}}(z)$ is the standard DGLAP branching kernel, $g(y)$ an approximate gluon PDF, and C gives an overall normalization of the companion distribution to unity. Furthermore an X rescaling is necessary as for valence quarks. The addition of a companion quark does break the momentum sum rule, this times upwards, and so is compensated by a scaling down of the gluon and sea PDFs.

In summary, in the downwards evolution, the kinematic limit is respected by a rescaling of x , as before. In addition the number of remaining valence quarks and new companion quarks is properly normalized. Finally, the momentum sum is preserved by a scaling of gluon and (non-companion) sea quarks. All of these scalings should not be interpreted as a physical change of the beam hadron, but merely as reflecting an increasing knowledge of its contents, akin to conditional probabilities.

At the end of the MPI + ISR generation sequence, a set of initiator partons have been taken out of the beam, *i.e.* partons that initiate the ISR chains that stretch in to the hard interactions. The beam remnant contains a number of leftover valence and companion quarks that carry the relevant flavour quantum numbers, plus gluons and sea to make up the total momentum. The latter are not book-kept explicitly, except for the rare case when the remnant contains no valence or companion quarks at all, and where a gluon is needed to carry the leftover momentum.

When the initiators are taken out of the incoming beam particle they are assumed to have a primordial k_{\perp} . Naively this would be expected to be of the order of the Fermi motion inside the proton, *i.e.* a few hundred MeV. In order to describe the low- p_{\perp} tail of the Z^0 spectrum a rather higher value of the order of 2 GeV seems to be required. This suggests imperfections in the modelling of ISR at small scales, specifically how and at what p_{\perp} scales it should be stopped. Also note that ISR dilutes the k_{\perp} at the hard interaction by a factor $x_{\text{hard}}/x_{\text{init}}$, *i.e.* by the fraction of the initiator longitudinal momentum that reaches the hard interaction. More ISR means a higher x_{init} and thus more dilution, counteracting the p_{\perp} gained by the ISR itself.

Given such considerations, a Gaussian distribution is used for the primordial k_{\perp} , with a width that depends on the scale Q (p_{\perp}) of each MPI, increasing smoothly from 0.36 GeV (= the string hadronization p_{\perp}) at small Q to 2 GeV at large. There is also a check that the k_{\perp} does not become too big for a low-mass system. The beam remnants are each given a k_{\perp} at the lower scale, but in addition they collectively have to take the recoil to ensure that the net p_{\perp} vanishes among the initiators and remnants.

The beam remnants also share leftover energy and longitudinal momentum. This is done by an ansatz of specific x spectra for valence quarks, valence diquarks, and companion quarks. The x values determine the relative fractions partons take of the lightcone momentum $E \pm p_z$, with + (−) for the beam moving in the $+z$ ($-z$) direction. It is not possible to fully conserve four-momentum inside each remnant + initiators system individually, however. Actually, by their relative motion the beam remnants together obtain a spectrum of invariant masses stretching well above the proton mass. Instead overall energy and momentum is preserved by longitudinal boosts of the two remnant subsystems, which effectively corresponds to a shuffling of four-momentum between the two sides. It is possible to generate too big remnant masses, but usually this can be fixed by a reselection of remnant x values.

What remains to consider is how the colours of partons are connected with each other to give the string pieces that eventually hadronize. This was one of the key stumbling blocks in the original model, especially what to do if several valence quarks are kicked out of a proton, Fig. 4. The main new tool at our disposal at this point is an implementation of junction fragmentation [118]. A junction is a vertex at which three string pieces come together, in a Y-shaped topology, and with each string stretching out to a quark, in the simplest case. The net baryon number then gets to be associated with the junction: given enough energy each string piece can break by the production of new $q\bar{q}$ (or $qq\bar{q}\bar{q}$) pairs, splitting off mesons (or baryon–antibaryon pairs), leaving the innermost q on each string to form a baryon together. An antijunction carries a negative baryon number, since the three strings in this case stretch out to antiquarks.

The rest frame of the junction is obtained in a symmetric configuration, where the opening angle between any pair of outgoing string ends is $2\pi/3 = 120^\circ$. This also defines the approximate rest frame of the central baryon. In cases where only one quark is kicked out of an incoming proton, the remaining two quarks in the beam remnant have a tiny opening angle in the collision rest frame, meaning the junction is strongly boosted in the forward direction, along with the two quarks, and these can then together be treated as a single unresolved diquark. If two valence quarks are kicked out, however, the junction can end up far away from the beam remnant itself. Note that a junction is normally not associated with the original quarks after a collision, owing to colour exchange.

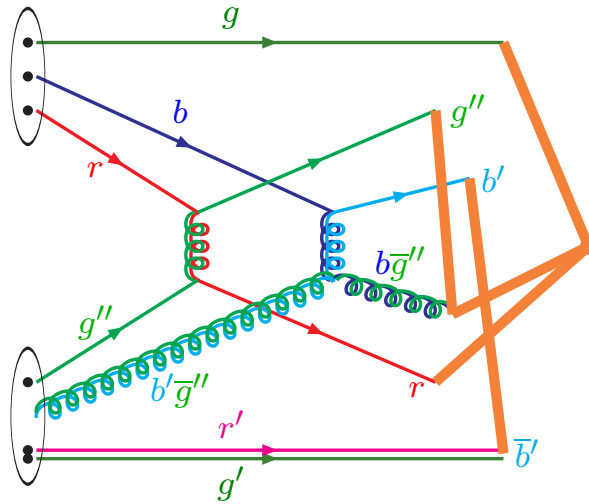


Figure 4: Example of an event where two valence quarks are kicked out from a proton, giving a junction topology. A possible colour flow is indicated, where primed colours are distinguishable from unprimed ones in the $N_C \rightarrow \infty$ limit. The remnant diquark is bookkept as a unit with $r' + g' = \bar{b}'$. Thick orange lines indicate strings stretched between outgoing partons, with the junction placed rightmost to avoid clutter.

A major complication is that the three strings may be stretched via various intermediate gluons out to the (new) endpoint quarks, and then the string motion and fragmentation becomes far more complex. It is such general issues that had taken time to resolve, at least approximately. Also systems containing a junction and an antijunction connected to each other need to be described.

Colours can be traced within each MPI individually, both through the hard interaction and the related ISR and FSR cascades, in the $N_C \rightarrow \infty$ limit [68]. If this limit is taken seriously, however, the beam remnants have to compensate the colours of all initiator partons, which means that they build up a high colour charge, which has to be carried by an unrealistically large number of remnant partons. It is more plausible, although a bit extreme in the other direction, to assume that the colour taken by one initiator is the anticolour of another one. It is such a strategy that allows us to work with the minimal number of beam remnants that preserves net flavour (or a single gluon if all valence quarks are kicked out). A sea quark initiator can be associated with its companion antiquark, be that another initiator or a remnant parton, and together be traced back to an imagined gluon that can be attached as above.

Thus only the valence colours remain. A proton can be described as a quark plus a diquark if none or one valence quark is kicked out, else as three quarks in a junction topology. It is along these original colour lines that the gluon initiators are attached one by one. Three main alternatives are implemented for the order of these attachments, from completely random to ones that favour smaller string lengths λ . (These connections can give a gluon the same colour as anticolour, which clearly is unphysical. Such colour associations are rejected and others tried.) Not even in the latter case does $\langle p_\perp \rangle (n_{\text{ch}})$ rise as fast as observed in the data, however, which suggests that a mere arrangement of colours in the initial state is not enough. A mechanism is also needed for CR in the final state, as already

used in the earlier models.

Again the λ measure is used to pick such reconnections: a string piece ij stretched between partons i and j and another mn between m and n can reconnect to in and mj if $\lambda_{in} + \lambda_{mj} < \lambda_{ij} + \lambda_{mn}$. A free strength parameter is introduced to regulate the fraction of pairs that are being tested this way. With this further mechanism at hand it now again becomes possible to describe $\langle p_{\perp} \rangle (n_{\text{ch}})$ data approximately.

7 Interleaved evolution

In models up until now, MPIs have been considered one by one. Once an MPI has been picked, the ISR and FSR associated with it has been generated before moving on to the next. This ordering is not trivial, since both the MPI and ISR mechanisms need to take momentum from the beam remnants, and therefore are in direct competition. If instead all MPIs had been generated first, and all ISR added only afterwards, the number of MPIs would have been higher and the amount of ISR less.

Time ordering does not give any clear guidance what is the correct procedure. We have in mind a picture where all MPIs happen simultaneously at the collision moment, while ISR stretches backwards in time from it, and FSR forwards. But we have no clean way of separating the hard interactions themselves from the virtual ISR cascades that “already” exist in the colliding hadrons.

Instead we choose the same guiding principle as we did when we originally decided to consider MPIs ordered in p_{\perp} : it is most important to get the hardest part of the story “right”, and then one has to live with an increasing level of approximation for the softer steps. With the introduction of p_{\perp} -ordered showers [119] it became possible to choose p_{\perp} as common evolution scale. Initially only MPI and ISR were interleaved, with FSR left to the end. This caught the important momentum competition between MPI and ISR, so was the big step. When PYTHIA 8 was written [120] full MPI/ISR/FSR interleaving [121] was default from the beginning. Going straight for the latter formulation, the scheme is characterized by one master formula

$$\begin{aligned} \frac{d\mathcal{P}}{dp_{\perp}} &= \left(\frac{d\mathcal{P}_{\text{MPI}}}{dp_{\perp}} + \sum \frac{d\mathcal{P}_{\text{ISR}}}{dp_{\perp}} + \sum \frac{d\mathcal{P}_{\text{FSR}}}{dp_{\perp}} \right) \\ &\times \exp \left(- \int_{p_{\perp}}^{p_{\perp\text{max}}} \left(\frac{d\mathcal{P}_{\text{MPI}}}{dp'_{\perp}} + \sum \frac{d\mathcal{P}_{\text{ISR}}}{dp'_{\perp}} + \sum \frac{d\mathcal{P}_{\text{FSR}}}{dp'_{\perp}} \right) dp'_{\perp} \right) \end{aligned} \quad (24)$$

that probabilistically determines what the next step will be. Here the ISR sum runs over all incoming partons, two per already produced MPI, the FSR sum runs over all outgoing partons, and $p_{\perp\text{max}}$ is the p_{\perp} of the previous step. Starting from the hardest interaction, Eq. (24) can be used repeatedly to construct a complete parton-level event.

Since each of the three terms contains a lot of complexity, with matrix elements, splitting kernels and PDFs in various combinations, it would seem quite challenging to pick a p_{\perp} according to Eq. (24). Fortunately the “winner-takes-it-all” trick (which is exact [122]) comes to the rescue. In it you select a $p_{\perp\text{MPI}}$ value as if the other terms did not exist in the equation, and correspondingly a $p_{\perp\text{ISR}}$ and a $p_{\perp\text{FSR}}$. Then the one of the three that is largest decides what is to come next. Inside the ISR and FSR sums one can repeat the

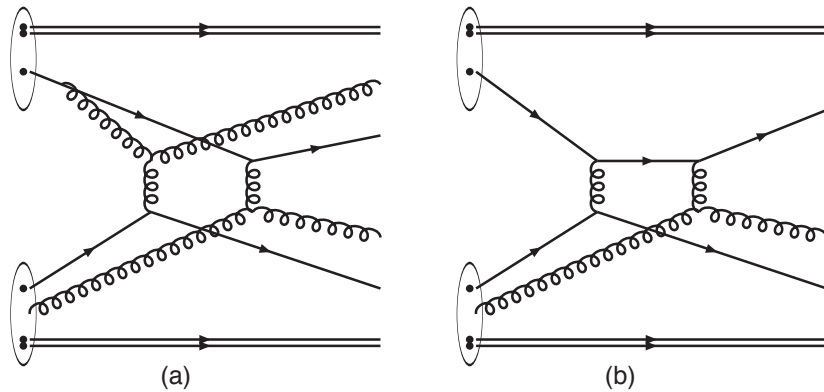


Figure 5: (a) Joined interactions. (b) Rescattering.

same trick, *i.e.* only consider one term at a time and decide which term gives the highest p_{\perp} .

The multiparton PDFs introduced in Sec. 6 play a key role, to help select a new MPI or perform ISR on an already existing one. Note that momentum and flavour should not be deducted for the current MPI itself when doing ISR. To exemplify, if the valence d quark has been kicked out of a proton in a given MPI, then there are no such d 's left for other MPIs, neither in ISR nor in MPI steps, but for the given MPI a valence d at higher x is still available as a potential mother to the current d .

In summary, p_{\perp} fills the function of a kind of factorization scale, where the perturbative structure above it has been resolved, while the one below it is only given an effective description *e.g.* in terms of multiparton PDFs. A decreasing p_{\perp} scale should then be viewed as an evolution towards increasing resolution; given that the event has a particular structure when viewed at some p_{\perp} scale, how might that picture change when the resolution cutoff is reduced by some infinitesimal dp_{\perp} ? That is, let the “harder” features of the event set the pattern to which “softer” features have to adapt.

8 Intertwined evolution

The above interleaving introduces a strong but indirect connection between different MPIs, in that each parton still has a unique association with exactly one MPI and its associated ISR and FSR. But this is likely not the full story; there are several ways in which the different MPIs may be much closer intertwined [123–126], see also [127]. The complexity then is significantly increased, and none of these further mechanisms are included by default in PYTHIA, but some have been studied and partly implemented.

The first possibility is joined interactions (JI) [119], Fig. 5(a). In it two partons participating in two separate MPIs may turn out to have a common ancestor when the backwards ISR evolution traces their prehistory. The joined interactions are well-known in the context of the forwards evolution of multiparton densities [128–132]. It can approximately be turned into a backwards evolution probability for a branching $a \rightarrow bc$

$$d\mathcal{P}_{bc}(x_b, x_c, Q^2) \simeq \frac{dQ^2}{Q^2} \frac{\alpha_s}{2\pi} \frac{x_a f_a(x_a, Q^2)}{x_b f_b(x_b, Q^2) x_c f_c(x_c, Q^2)} z(1-z) P_{a \rightarrow bc}(z), \quad (25)$$

with $x_a = x_b + x_c$ and $z = x_b/(x_b + x_c)$. The main approximation is that the two-parton differential distribution has been factorized as $f_{bc}^{(2)}(x_b, x_c, Q^2) \simeq f_b(x_b, Q^2) f_c(x_c, Q^2)$ to put the equation in terms of more familiar quantities.

Just like for the other processes considered, a form factor is given by integration over the relevant Q^2 range and exponentiation. Associating $Q \simeq p_\perp$, as is already done for normal ISR, Eq. (25) can be turned into a $\sum d\mathcal{P}_{\text{JI}}/dp_\perp$ term that can go into Eq. (24) along with the other three. The JI sum runs over all pairs of initiator partons with allowable flavour combinations, separately for the two incoming hadrons. A gluon line can always be joined with a quark or another gluon one, and a sea quark and its companion can be joined into a gluon. The parton densities are defined in the same spirit as before, *e.g.* $f_b(x_b, p_\perp^2)$ and $f_c(x_c, p_\perp^2)$ are squeezed to be smaller than X , where X is reduced from unity by the momentum carried away by all but the own interaction, and for $f_a(x_a, p_\perp^2)$ by all but the b and c interactions.

Technical complications arise when the kinematics of JI branchings has to be reconstructed, notably in transverse momentum, and the code to overcome these was never written. The reason is that already the evolution itself showed that JI effects are small. Most events do not contain any JI at all above the ISR cutoff scale, and in those that do the JI tends to occur at a low p_\perp value. There are two reasons for this. One is numerical: the number of parton pairs that can be joined increases as more MPIs have already been generated. The other is the PDF behaviour: for all but the smallest $Q^2 = p_\perp^2$ scales the huge number of small- x gluons and sea quarks dominate, and it is only close to the lower evolution cutoff that the few valence quarks and high- x gluons play an increasingly important role in the ISR backwards evolution.

The second intertwining possibility is rescattering, *i.e.* that a parton from one incoming hadron consecutively scatters against two or more partons from the other hadron, Fig. 5(b). The simplest case, $3 \rightarrow 3$, *i.e.* one rescattering, has been studied [30,31,34]. The conclusion is that it should be less important than two separated $2 \rightarrow 2$ processes: $3 \rightarrow 3$ and $2 \times (2 \rightarrow 2)$ contain the same number of vertices and propagators, but the latter wins by involving one parton density more. The exception could be large p_\perp and x values, but there $2 \rightarrow n, n \geq 3$ QCD radiation anyway is expected to be the dominant source of multijet events.

For rescattering, a detailed implementation is available as an option in PYTHIA [122], as follows. Previously we have described how partons are taken out of the conventional PDFs after each MPI (and ISR), such that less and less of the original momentum remains. If we now should allow a rescattering then a scattered parton has to be put back into the PDF, but now as a δ function. It can be viewed as a quantum mechanical measurement of the wave function of the incoming hadron, where the original ‘‘squared wave function’’ $f(x, Q^2)$ in part collapses by the measurement process of one of the partons in the hadron. That is, one degree of freedom has now been fixed, while the remaining ones are still undetermined. A hadron can therefore be characterized by a new PDF

$$f(x, Q^2) \rightarrow f_{\text{rescaled}}(x, Q^2) + \sum_i \delta(x - x_i) = f_u(x, Q^2) + f_\delta(x, Q^2), \quad (26)$$

where f_u represents the unscattered part of the hadron and f_δ the scattered one. The scattered partons have the same x values as originally picked, in the approximation that small-angle t -channel gluon exchange dominates, but more generally there will be shifts.

The sum over delta functions runs over all partons that are available to rescatter, including outgoing states from hard or MPI processes and partons from ISR or FSR branchings. All the partons of this disturbed hadron can scatter, and so there is the possibility for an already extracted parton to scatter again.

With the PDF written in this way, the original MPI probability in Eq. (24) can now be generalised to include the effects of rescattering

$$\frac{d\mathcal{P}_{\text{MPI}}}{dp_{\perp}} \rightarrow \frac{d\mathcal{P}_{\text{uu}}}{dp_{\perp}} + \frac{d\mathcal{P}_{\text{u}\delta}}{dp_{\perp}} + \frac{d\mathcal{P}_{\delta\text{u}}}{dp_{\perp}} + \frac{d\mathcal{P}_{\delta\delta}}{dp_{\perp}}, \quad (27)$$

where the uu component represents the original MPI probability, the u δ and δ u components a single rescattering and the $\delta\delta$ component a double rescattering. In this way, rescattering interactions are included in the common p_{\perp} evolution of MPI, ISR and FSR.

Again the evolution in p_{\perp} should be viewed as a resolution ordering. In a time-ordered sense, a parton could scatter at a high p_{\perp} scale and rescatter at a lower one, or the other way around, with comparable probabilities. To simplify the already quite complicated machinery, it is chosen to set up the generation as if the rescattering occurs both at a lower p_{\perp} and a later time than the “original” scattering, while retaining the full rescattering rate.

In simple low-angle scatterings there is a unique assignment of scattered partons to either of the two colliding hadrons A and B , but for the general case this is not so simple. Different prescriptions have been tried, including the most extreme where all scattered partons can scatter again against partons from either beam. It turns out that differences are small for single rescatter. The scheme dependence is bigger for double rescattering, but this process is anyway significantly suppressed relative to the single rescatters.

The real problem, however, is how to handle kinematics when ISR, FSR and primordial k_{\perp} are added to rescattering systems. To propagate recoils between systems that are partly intertwined but also partly separate requires what is the most nontrivial code in the whole PYTHIA MPI framework, and it would carry too far to describe it here.

More important are the results. At the LHC we predict that of the order of half of all minimum-bias events contains at least one rescattering, and for events with hard processes the fraction is even larger. Double rescattering is rare, however, and can be neglected. Evaluating the consequences of rescattering is still challenging, since it is a secondary effect within the MPI machinery. The precise amount of MPI has to be tuned to data, *e.g.* by varying the $p_{\perp 0}$ turn-off parameter, so the introduction of rescattering to a large extent can be compensated by a slight decrease in the amount of “normal” $2 \rightarrow 2$ MPIs. Worse still, most MPIs are soft to begin with, and rescattering then introduces a second scale, even softer than the “original” scattering. Thus, rescattering is typically associated with particle production at the lower limit of what can be reliably detected. There are some effects of the Cronin type [133] in hadronic p_{\perp} spectra, *i.e.* a shift towards higher p_{\perp} , but too small to offer a convincing signal.

If one zooms in on the tail of events at larger scales, the rate of (semi-)hard three-jet events from rescattering is of the same order in α_s as four-jets from DPS, but the background from ISR and FSR starts one order earlier for three-jets. Furthermore, DPS has some obvious characteristics to distinguish it from $2 \rightarrow 4$ radiation topologies: pairwise balanced jets with an isotropic relative azimuthal separation. No corresponding unique kinematic features are expected for $3 \rightarrow 3$ rescattering vs. $2 \rightarrow 3$ ISR/FSR, and we have not found any either. Hopefully smarter people will one day find the right observable.

The third and most dramatic intertwining possibility is that the perturbative cascades grip into each other. An example is the “swing” mechanism, whereby two dipoles in the initial state can reconnect colours, which is a key aspect of the DIPSY generator [134,135], see also [136]. Currently there is no mechanism of this kind in PYTHIA.

9 An x -dependent impact-parameter profile

As described in Sec. 4, a double Gaussian impact-parameter profile was the initial choice, and remained the default for many years. With the introduction of full ISR/FSR in all MPIs, Sec. 6, a single Gaussian is almost giving enough fluctuations. The “hot spots”, that the double Gaussian was introduced to represent, now are obtained in part by the ISR/FSR cascades associated with each MPI, with somewhat fewer separate MPIs needed for the same overall activity. Put another way, the varying ISR/FSR activity introduces another mechanism for fluctuations, while a smaller $\langle n_{\text{MPI}} \rangle$ means that the scaled width $\sigma_{\text{MPI}}(b)/\langle n_{\text{MPI}}(b) \rangle$ goes up, both reducing the need for broader-than-Gaussian profiles.

Given the reduced sensitivity to non-Gaussian profiles, a one-parameter alternative was therefore introduced

$$\tilde{\mathcal{O}}(b) = \exp(-b^d) , \quad (28)$$

where $d < 2$ gives more fluctuations than a Gaussian and $d > 2$ less. Do note that the expression is for the overlap, not for the individual hadrons, for which no simple analytical form is available.

One aspect, however, is that we have assumed the transverse b profile to be decoupled from the longitudinal x one. This is not the expected behaviour, because low- x partons should diffuse out in b during the evolution down from higher- x ones [137], see also [138]. Additionally, if $b = 0$ is defined as the center of energy of a hadron, then by definition a parton with $x \rightarrow 1$ also implies $b \rightarrow 0$.

Such diffusion was already studied in Sec. 5. In the later study [139], described here, there was no attempt to trace the evolution of cascades in x . Rather it is assumed that the b distribution of partons at any x can be described by a simple Gaussian, but with an x -dependent width:

$$\rho(r, x) \propto \frac{1}{a^3(x)} \exp\left(-\frac{r^2}{a^2(x)}\right) \quad \text{with} \quad a(x) = a_0 \left(1 + a_1 \ln \frac{1}{x}\right) , \quad (29)$$

with a_0 and a_1 to be determined. The overlap is then given by

$$\tilde{\mathcal{O}}(b, x_1, x_2) = \frac{1}{\pi} \frac{1}{a^2(x_1) + a^2(x_2)} \exp\left(-\frac{b^2}{a^2(x_1) + a^2(x_2)}\right) . \quad (30)$$

In principle one could argue that also a third length scale should be included, related to the transverse distance the exchanged propagator particle, normally a gluon, could travel. This distance should be made dependent on the p_{\perp} scale of the interaction. For simplicity this further complication is not considered but, on the other hand, a finite effective radius is allowed also for $x \rightarrow 1$. The $x \rightarrow 1$ limit is not much probed in MB, since the bulk of MPIs occur at small x , but can be relevant for UE studies, *e.g.* for the production of new particles at high mass scales.

The two parameters a_0 and a_1 could be tuned at each CM energy. One combination of them is fixed so as to reproduce σ_{nd} . If the wider profile of low- x partons is related to the growth of $\sigma_{\text{nd}}(s)$, then a_1 can be constrained by the requirement that a_0 should be independent of energy. This is reasonably well fulfilled for $a_1 = 0.15$, which is therefore taken as default in this scenario.

The generation of events is more complicated with an x -dependent overlap, but largely involves the same basic principles. Again the b value of an event is selected in conjunction with the kinematics of the hardest interaction, and is thereafter fixed. The acceptance of subsequent MPIs is proportional to $\tilde{\mathcal{O}}(b, x_1, x_2)$, where x_1 and x_2 are the values for the MPI under consideration.

In overall MB and UE phenomenology, the scenario with $a_1 = 0.15$ ends up roughly halfway between the single and double Gaussian ones. It depends on the process under consideration, however. A 10 GeV γ^* would give an MPI activity close to the single Gaussian, while a 1 TeV Z' would have markedly higher MPI activity, since larger x values would be accessed in the latter process.

Unfortunately, in the experimental tunes to MB and UE data that were made to this model variant [140], no convincing evidence were found for an $a_1 > 0$. A dedicated study of how the UE varies as a function of the mass of $\mu^+\mu^-$ pairs could provide the definitive test.

10 Diffraction

The nature of diffraction is not obvious, and has been addressed from different points of view over the years, see [15]. From the perspective of this article the story begins with the Ingelman–Schlein model [141], wherein it is assumed that the exchanged Pomeron \mathbb{P} can be viewed as a hadronic state, and that therefore the creation of a diffractive system can be described as a hadron-hadron collision. This implies that the \mathbb{P} has PDFs, which enables hard processes to occur, as was confirmed by the observation of jet production in diffractive systems [142]. The POMPYT program [143] combined the \mathbb{P} flux inside the proton with the \mathbb{P} PDFs, both largely determined from HERA data, and used PYTHIA to produce complete hadronic final states.

Originally PYTHIA itself had a more primitive description, based on a purely longitudinal structure of the diffractive system, for single diffraction either stretched between a kicked-out valence quark and a diquark remnant, or stretched in a hairpin configuration with a kicked-out gluon connected to both a quark and a diquark in the remnant. This was sufficient for low-mass diffraction, but clearly not for high-mass one. Therefore a complete MPI machinery was implemented [121, 144]. The diffractive mass is selected as a first step. Thereafter \mathbb{P} and ordinary p PDFs are used to generate an ordinary sequence of MPIs.

There are some catches, however. One is that \mathbb{P} PDFs often are not normalized to unit momentum, in part based on theoretical arguments but mainly because what hard processes probe is the convolution of \mathbb{P} flux and PDFs, not each individually. For the handling of momentum conservation issues in a generator, however, it is essential to let the MPI machinery have access to properly rescaled PDFs, as in Sec. 6, and for that an implicit normalization to unity is used. Another is that the MPI machinery also requires a normalization to an effective $\sigma_{\mathbb{P}p}$, to replace the σ_{nd} used for normal nondiffractive events,

starting from Eq. (4). Again this is not directly measurable, so a default value of 10 mb has been chosen to give $\mathbb{P}p$ properties, such as $\langle n_{\text{ch}} \rangle$, comparable with $pp/p\bar{p}$ at the same mass.

The diffractive machinery generates a mass spectrum that stretches down to ~ 1.3 GeV, but obviously it is not possible to apply an MPI philosophy that low. Therefore, below 10 GeV, the original longitudinal description is recovered. At low masses the kicked-out valence quark scenario is assumed to dominate, but then fall off in favour of a kicked-out gluon. Above 10 GeV there is a transition region, wherein the MPI description gradually takes over from the longitudinal one.

In its details several further deliberations and parameters are involved. There is also a somewhat separate MBR model [145] as an option.

Diffraction raises more MPI questions. In the collision of two incoming protons, one \mathbb{P} exchange could imply a diffractive topology with a rapidity gap, but other simultaneously occurring MPIs would fill in that gap and produce an ordinary MB event. A spectacular example is Higgs production by gauge-boson fusion, $W^+W^- \rightarrow H^0$ and $Z^0Z^0 \rightarrow H^0$, where the naive process should result in a large central gap only populated by the Higgs decay products, since no colour exchange is involved. Including MPIs, this gap largely fills up [146], although a fraction of the events should contain no further MPIs [147], a fraction denoted as the Rapidity Gap Survival Probability. Such a picture has been given credence by the observation of “factorization breaking” between HERA and the Tevatron: the \mathbb{P} flux and PDFs determined at HERA predict about an order of magnitude more QCD jet production than observed at the Tevatron [148].

In a recent study [149] a dynamical description of such factorization breaking is implemented, as a function of the hard-process kinematics, to predict the resulting event structure for hard diffraction in hadronic collisions. This is done in three steps. Firstly, given a hard process which has been selected based on inclusive PDFs, the fraction of a PDF that should be associated with diffraction is calculated, obtained as a convolution of the \mathbb{P} flux and its PDFs. Secondly, the full MPI framework of PYTHIA, including also ISR and FSR effects, is applied to find the fraction of events without any further MPIs. Those events that survive these two steps define the diffractive event fraction, while the rest remain as regular nondiffractive events. Thirdly, diffractive events may still have MPIs within the $\mathbb{P}p$ subsystem, and therefore the full hadron-hadron underlying-event generation machinery is repeated for this subsystem. The nondiffractive events are kept as they are in this step.

For typical processes, such as QCD jets or Z^0 production, the PDF step gives $\sim 10\%$ of the events to be of diffractive nature. The requirement of having no further MPIs gives an approximate factor of 10 further suppression, so that only around 1% of the processes show up as diffraction. These numbers are in overall agreement with the experimental ones, but the availability of a complete implementation should allow more detailed tests. Unfortunately there is still a non-negligible uncertainty, both for the model itself and for the external input, such as \mathbb{P} PDFs.

11 Colour reconnection

Colour reconnection is a research field on its own, although tightly connected to MPIs, and has been reviewed elsewhere [150, 151]. Here only some brief notes follow, again with emphasis on PYTHIA aspects.

As mentioned in Sec. 4, CR was essential to obtain a rising $\langle p_{\perp} \rangle(n_{\text{ch}})$, and that has remained a constant argument over the years, still valid today: separate MPIs must be colour-connected in such a way that topologies with a reduced λ measure, Eq. (18), are favoured.

LEP 2 offered a good opportunity to search for CR effects. Specifically, in a process $e^+e^- \rightarrow W^+W^- \rightarrow q_1\bar{q}_2q_3\bar{q}_4$, CR could lead to the formation of alternative “flipped” singlets $q_1\bar{q}_4$ and $q_3\bar{q}_2$, and correspondingly for more complicated parton/string topologies. Such CR would be suppressed at the perturbative level, since it would force some W propagators off the mass shell. This suppression would not apply in the soft region. Two main models were developed in the PYTHIA context [152]. Strings are viewed as elongated bags in scenario I, and reconnection is proportional to the space–time overlap of these bags. In scenario II, strings are instead imagined as vortex lines, and two cores need to cross each other for a reconnection to occur. In either case it is additionally possible to allow only reconnections that reduce λ , scenarios I' and II'. Based on a combination of results from all four LEP collaborations, the no-CR null hypothesis is excluded at 99.5% CL [153]. Within scenario I the best description is obtained for $\sim 50\%$ of the 189 GeV W^+W^- events being reconnected, in qualitative agreement with the PYTHIA predictions.

Unfortunately it is more difficult to formulate a similarly detailed model of the space–time picture of hadronic collisions, and this has not been done for PYTHIA. (In part such pictures are presented *e.g.* in DIPSY and EPOS.) Instead simpler scenarios for reducing the λ have been used. In total PYTHIA 6 came to contain twelve models, many of them involving annealing strategies.

The current PYTHIA 8 [154] initially only contained one model, which still is the default. In it two MPIs can be merged with a probability $\mathcal{P} = r^2 p_{\perp 0}^2 / (r^2 p_{\perp 0}^2 + p_{\perp \text{lower}}^2)$, where r is a free parameter, $p_{\perp 0}$ is the standard dampening scale of MPIs, and $p_{\perp \text{lower}}$ is the scale of the lower- p_{\perp} MPI. Each gluon of the latter MPI is put where it increases λ the least for the higher- p_{\perp} MPI. The procedure is applied iteratively, so for any MPI the probability of being reconnected is $\mathcal{P}_{\text{tot}} = 1 - (1 - \mathcal{P})^{n_{>}}$, where $n_{>}$ is the number of MPIs with higher p_{\perp} .

A new QCD-based CR model [155] implements a further range of reconnection possibilities, notably allowing the creation of junctions by the fusion of two or three strings. The relative rate for different topologies is given by SU(3) colour rules in combination with a minimization of the λ measure. The many junctions leads to an enhanced baryon production, although partly compensated by a shift towards strings with masses too low for baryon production.

A specific application of CR is for t , Z^0 and W^{\pm} decays. With widths around 2 GeV, *i.e.* $c\tau \approx 0.1$ GeV, their decays happen after other hard perturbative activity (ISR/FSR/MPI) but still inside the hadronization colour fields, thereby allowing CR with the rest of the event. It was already for the Tevatron noted that this is a non-negligible source of uncertainty in top mass determinations [156], and for similar LHC studies several new CR models were implemented in PYTHIA 8 [157]. These fall in two classes: either the t and W decay products undergo CR on equal footing with the rest of the event, or their decays and

CR are considered after the rest of the partonic event has had a chance to reconnect. The latter scenario allows more flexibility, to explore also extreme possibilities.

12 LHC lessons

LHC has been very productive in presenting data of relevance for MB/UE/MPI/DPS studies, and there is no possibility to cover even a fraction of it here. The following therefore is a very subjective selection.

To begin with, some words on tunes, see also [9, 158]. Generators contain a large number of free parameters, by necessity, that attempt to parametrize our ignorance. Many of these are correlated, so cannot be determined separately. A tune is then the outcome of an effort to determine a set of key parameters simultaneously. This is an activity that generator authors do at a basic level all the time, and occasionally as a more concerted effort, *e.g.* [121, 159–161]. It is also an activity that experimental collaborations undertake, given the direct access to data and the needs of their communities. With no claims of completeness, the PYTHIA 6 code contains settings for more than 100 different tunes, *e.g.* [82, 83, 162–164], whereof about half precede the LHC startup, and the PYTHIA 8 one for 34 so far, *e.g.* [140, 165–167]. Many of these are minor variations around a common theme. Some tunes have been made by hand whereas others use automated procedures such as PROFESSOR [168]. The access to validated RIVET analysis routines [169] have played an increasingly important role. Data comparisons for many tunes are available in MCPLOTS [170].

Whereas theorists aim for the best overall description, experimentalists often produce separate MB and UE tunes. With less data to fit, it is possible to obtain a better description for the intended applications. So far it has not been settled how much of the differences in MB and UE parameters represent true shortcomings of the model and how much is a consequence of the fitting process itself.

Several PYTHIA 6 tunes served as a basis for predictions prior to the LHC startup. Early 7 TeV data showed that most of them undershot the level of activity by some amount, with one being close, but none above. Fortunately a modest change of the energy dependence of the $p_{\perp 0}$ is enough to bring up the activity to a reasonable level, and further extrapolations to 13 TeV have worked better.

Generally speaking, PYTHIA has been able to explain most phenomenology observed at LHC so far, at least qualitatively, and often also quantitatively. Nevertheless, a significant number of observations do not look as nice. A common theme for many of them is that high-multiplicity pp events have properties similar to those observed in heavy-ion AA collisions. Examples are [171]

- High-multiplicity events have a higher fraction of heavier particles, notably multi-strange baryons [172], whereas the composition stays rather constant in PYTHIA.
- The $\langle p_{\perp} \rangle$ is larger for heavier particles [173] (also observed at RHIC [174]), more so than PYTHIA predicts.
- The charged particle p_{\perp} spectrum is underestimated at low p_{\perp} scales [175–177], *e.g.* leading to problems in simultaneously fitting MB data analyzed with $p_{\perp} > 0.1$ GeV and $p_{\perp} > 0.5$ GeV. The deficit is mainly associated with too little π^{\pm} production [178].
- The Λ/K spectrum ratio has a characteristic peak at around 2.5 GeV [179], which is

not at all reproduced.

- The observation of a ridge in two-particle correlations, stretching out in rapidity on both sides of a jet peak, especially for high-multiplicity events [180–182]. Correlation functions also points to azimuthal flow, similarly to AA observations.

An alternative model has been formulated [171] to explore at least some of these discrepancies, with three main deviations from the standard framework. Firstly the standard Gaussian p_{\perp} spectrum for primary hadron production is replaced by an exponential one, $\exp(-m_{\perp\text{had}}/T)$. It is loosely inspired by thermodynamics, with T an effective temperature, and is intended to enhance the pion rate at small p_{\perp} , while increasing $\langle p_{\perp} \rangle$ for heavier particles. Secondly, it is assumed that the normal string tension, alternatively the T above, is increased in regions of phase space where strings are close-packed, which typically is caused by a high MPI activity. This is intended to change both particle composition and p_{\perp} spectra. Thirdly, a simple model for hadronic rescattering is introduced, whereby hadrons tend to obtain more equal velocities, *i.e.* larger $\langle p_{\perp} \rangle$ for heavier particles.

Unfortunately, effects are not as large as one might hope. Specifically, most pions come from decays of heavier hadrons, and so the mechanisms intended to give less p_{\perp} to pions and more to kaons and protons are counteracted. Nevertheless the thermodynamical model is able to provide significantly improved descriptions of observables such as the p_{\perp} spectrum of charged hadrons, the average transverse momentum as a function of the hadron mass, and the enhanced production of strange hadrons at large multiplicities.

Even more successful are the DIPSY and EPOS generators, however. In DIPSY dense string packing is assumed to lead to the formation of colour ropes [135], wherein an increased string tension favours the production of heavier hadrons and larger p_{\perp} values, and a shoving mechanism can induce ridge and related phenomena [183]. In EPOS the central region of pp collisions can form a quark–gluon plasma, which also allows strangeness enhancements, and strings in the outer regions can again be shoved by the central pressure, to give ridges [114].

These new data, and the models they favour, may have consequences for the way we think about MPIs. Having MPIs as the origin of QGP formation in AA is an old idea [184], but now it might even apply to pp . One could also note that the rising trend of $\langle p_{\perp} \rangle(n_{\text{ch}})$, once the key reason to introduce CR, now partly might be attributed to collective effects.

13 Current state of the PYTHIA MPI machinery

The MPI machinery implemented in PYTHIA has evolved over the years, as we have seen. It is therefore useful to make a quick rundown of the current state, and also mention a few odds and ends that were not yet covered.

The starting point is to define a $d\sigma/dp_{\perp}^2$, Eq. (2), that decides which processes can occur in an MPI, and then also occurs in the Sudakov-like factor. Originally it only contained QCD $2 \rightarrow 2$ processes, but now also includes $2 \rightarrow 2$ with photons in the final state, or mediated by an s -channel γ^* , or by t -channel $\gamma^*/Z^0/W^{\pm}$ exchange, or charmonium and bottomonium production via colour singlet and octet channels. This combined cross section is then regularized in the $p_{\perp} \rightarrow 0$ limit by the damping factor in Eq. (8).

There are two main options to begin the generation. One is if a hard process already has been selected, with a generic hardness scale, *e.g.* the factorization scale, which we for the sake of bookkeeping equate with $p_{\perp 1}$. Then the impact parameter b can be selected

according to one of five possibilities: no b dependence, single Gaussian, double Gaussian, $\exp(-b^p)$ overlap and x -dependent Gaussian. The other main option is *e.g.* for inclusive non-diffractive production, where $p_{\perp 1}$ and b have to be selected correlated according to Eq. (15). (Also with an explicit x_1, x_2 dependence for the x -dependent Gaussian.)

The downwards evolution in p_{\perp} can then proceed, Eq. (17). For a preselected hard process there is an ambiguity, however, whether to allow $p_{\perp 2}$ to be restricted by $p_{\perp 1}$ or go all the way up to the kinematic limit. The former is required for QCD jets, to avoid double-counting, while the latter would be sensible for more exotic processes, where there is no such risk. By default PYTHIA will make this decision based on some simple rules, but it is also possible to choose strategy explicitly.

The downwards evolution of MPIs is interleaved in p_{\perp} with ISR and FSR, Eq. (24). Optionally one may also include rescattering in the MPI framework, Eq. (27), but this comes at a cost, so is not recommended for normal usage. Joined interactions are not implemented in the PYTHIA 8 code, and there is also no swing mechanism.

Modified multiparton PDFs during the evolution follow the strategy of Sec. 6. The same section also describes the related handling of beam remnants. The subsequent colour reconnection stage allows for several different models, with many options. String fragmentation and decays is added at the end of the generation chain, with junction topologies playing a key role for the preservation of the incoming baryon numbers.

Diffractive topologies are included in a picture where the Pomeron is given a hadronic substructure, implying that $\mathbb{P}p$ and $\mathbb{P}\mathbb{P}$ subcollisions should be handled with a full MPI machinery of its own, at least for higher diffractive masses.

In total, essentially all the questions raised about the original model, end of Sec. 3, have since been studied, and tentative answers have been implemented in the existing code.

The generation of DPS is implicit in the MPI machinery. Whereas the first interaction can always be selected hard, normally the second one would tend to be soft. There is a special machinery in PYTHIA to generate two hard interactions. To understand how it operates, start from the Poissonian distribution $\mathcal{P}_n = \langle n \rangle^n \exp(-\langle n \rangle) / n!$. If $\langle n \rangle \ll 1$, as it should be for a hard process, the exponential can be neglected and $\mathcal{P}_2 = \langle n \rangle^2 / 2$. Now imagine two processes a and b with cross sections σ_a and σ_b , meaning that they are produced with rates $\langle n_a \rangle = \sigma_a / \sigma_{\text{nd}}$ and $\langle n_b \rangle = \sigma_b / \sigma_{\text{nd}}$ inside the inelastic event class. Then the cross section for having two such MPIs is

$$\sigma_2 = \sigma_{\text{nd}} \mathcal{P}_2 = \sigma_{\text{nd}} \frac{(\langle n_a \rangle + \langle n_b \rangle)^2}{2!} = \frac{\sigma_a^2 + 2\sigma_a\sigma_b + \sigma_b^2}{2\sigma_{\text{nd}}} \quad (31)$$

The above equation neglects the impact-parameter dependence. A hard collision implies a smaller average b than for MB events, as we have discussed before, and thus an enhanced rate for the second collision. Poissonian statistics applies for a fixed b , but when averaging over all b an enhancement factor \mathcal{E} is generated. Conventionally such effects are included by replacing the final σ_{nd} in Eq. (31) by an σ_{eff} . Unintuitively a lower σ_{eff} corresponds to a higher \mathcal{E} . It can be written as [185]

$$\mathcal{E} = \frac{\sigma_{\text{nd}}}{\sigma_{\text{eff}}} = \frac{\int \tilde{\mathcal{O}}^2(b) d^2b \times \int \mathcal{P}_{\text{int}}(b) d^2b}{\left(\int \tilde{\mathcal{O}}(b) d^2b \right)^2}. \quad (32)$$

Thus \mathcal{E} depends on the shape of $\tilde{\mathcal{O}}(b)$, with a distribution more spiked at $b = 0$ giving a larger \mathcal{E} . But \mathcal{E} also depends on the CM energy and the $p_{\perp 0}$ scale, which enter via $\mathcal{P}_{\text{int}}(b)$.

There is also a dynamical depletion factor related to PDF weights. With the two hard processes initially generated independently of each other, flavour and momentum constraints are not taken into account. Therefore, afterwards, PDFs are re-evaluated as if either interaction were the first one, giving modified PDFs for the second one, as described in Sec. 6. The average PDF weight change of the two orderings is used as extra event weight, leading to some configurations being rejected.

The program allows the two hard interactions to be selected in partly overlapping channels, and/or (with some warnings) phase space regions. Assume *e.g.* that process 1 can be either *a* or *c* and process 2 either *b* or *c*. Then an extension of Eq. (31) tells us the numerator should be

$$2\sigma_{1a}\sigma_{2b} + 2\sigma_{1a}\sigma_{2c} + 2\sigma_{1c}\sigma_{2b} + \sigma_{1c}\sigma_{2c} = 2(\sigma_{1a} + \sigma_{1c})(\sigma_{2b} + \sigma_{2c}) - \sigma_{1c}\sigma_{2c} \quad (33)$$

To obtain the correct answer the prescription is thus to generate process 1 according to $\sigma_a + \sigma_c$ and process 2 according to $\sigma_b + \sigma_c$, but to throw half of those events where both 1 and 2 were picked to be process *c*.

14 Summary and Outlook

In this chapter we have traced the evolution of MPI ideas in PYTHIA over more than 30 years. The emphasis has been on the early developments, since that set the stage for what has come later, and more generally on the theoretical ideas and concepts that have been explored over the years. It is intended to offer a complementary view to other chapters in this book, and so we have avoided detailed comparisons with data, and also not gone into details of other models.

By and large, the original MPI ideas have stood the test of time; they are still at the core of the current PYTHIA framework. The further work that has been done since is much more extensive than the original one, but often suffers from diminishing returns, *i.e.* that major upgrades only moderately improve the general agreement with data. Nevertheless it is important to explore as many aspects of MPIs as possible. They do encode important information on the borderline between perturbative and nonperturbative physics, and we should become better at decoding this information.

The PYTHIA development described here has been very much influenced by perceived experimental needs, and inspired by theoretical ideas, but has been decoupled from detailed theoretical calculations. The reason is obvious: already DPS offers a formidable challenge, enough to keep theorists busy, and so useful results for truly *multiparton* interactions are rare. While it is interesting to understand two-parton PDFs better, say, in PYTHIA we need to be able to address twenty-parton PDFs, and nothing less will do.

In this spirit it is important to recall that, even though studies of DPS is an important way to explore MPI, it is not the only one. An example on the to-do list is the lumpiness of particle production in general, *e.g.* as probed by the minijet rate for different jet clustering *R* and $p_{\perp\min}$ parameter values, down to the $p_{\perp 0} \approx 2.5$ GeV scale (at LHC energies). And it should not be forgotten that (for some people, like me) the most convincing — and earliest — evidence of MPIs is the broadness of multiplicity distributions. The intermittency [186, 187] interpretations of multiplicity fluctuations at the $S\bar{p}\bar{p}S$ [188, 189] may have been

over-enthusiastic at times, but more parts of the same experimental program could be carried out at the LHC and yield useful results.

Nevertheless, the LHC has provided new impetus to the whole MB/UE field of studies, by the observation of new and unexpected phenomena. Both the ridge effect and the enhancement of multi-strange baryons in high-multiplicity events, to take the two most spectacular examples, remain to be fully understood. These observations do not invalidate the MPI concept. On the contrary, plausible explanations start out from a MPI picture and add some kind of collective behaviour among the MPIs. Colour ropes or other ways to obtain an increased string tension is one example, the formation of a quark-gluon-plasma-like (multiparton!) state another.

Clearly much work lies ahead of us to fully understand what has already been observed, and hopefully also many further surprises will come along to stimulate us further.

Acknowledgements

Thanks to all collaborators on MPI physics through the years, and to Jonathan Gaunt and Peter Skands for helpful comments on the draft manuscript. This project has received funding in part by the Swedish Research Council, contracts number 621-2013-4287 and 2016-05996, in part from the European Research Council (ERC) under the European Union's Horizon 2020 research and innovation programme (grant agreement No 668679), and in part through the European Union Marie Curie Initial Training Networks MCnetITN PITN-GA-2012-315877 and MCnetITN3 722104.

References

- [1] H. U. Bengtsson, "The Lund Monte Carlo for High p_T Physics," *Comput. Phys. Commun.* **31** (1984) 323.
- [2] B. Andersson, G. Gustafson, G. Ingelman, and T. Sjöstrand, "Parton Fragmentation and String Dynamics," *Phys. Rept.* **97** (1983) 31–145.
- [3] B. Andersson, G. Gustafson, and T. Sjöstrand, "How to Find the Gluon Jets in e^+e^- Annihilation," *Phys. Lett.* **B94** (1980) 211–215.
- [4] **JADE** Collaboration, W. Bartel *et al.*, "Experimental Study of Jets in electron - Positron Annihilation," *Phys. Lett.* **B101** (1981) 129–134.
- [5] T. Sjöstrand, "The Lund Monte Carlo for Jet Fragmentation," *Comput. Phys. Commun.* **27** (1982) 243.
- [6] T. Sjöstrand, "A Model for Initial State Parton Showers," *Phys. Lett.* **B157** (1985) 321–325.
- [7] T. Sjöstrand, "Multiple Parton-Parton Interactions in Hadronic Events." Oregon Workshop on Super High Energy Physics, FERMILAB-PUB-85-119-T, 1985.

- [8] T. Sjöstrand and M. van Zijl, “A Multiple Interaction Model for the Event Structure in Hadron Collisions,” *Phys. Rev.* **D36** (1987) 2019.
- [9] S. Bansal, D. Kar, and R. Field. this book.
- [10] I. Belyaev. this book.
- [11] P. Gunnellini. this book.
- [12] O. Gueta. this book.
- [13] A. O. Velasquez. this book.
- [14] M. Floris and L. Wei. this book.
- [15] F. Hautmann and H. Jung. this book.
- [16] J. F. Grosse-Oetringhaus. this book.
- [17] **UA5** Collaboration, G. J. Alner *et al.*, “Scaling Violation Favoring High Multiplicity Events at 540-GeV CMS Energy,” *Phys. Lett.* **B138** (1984) 304–310.
- [18] **UA5** Collaboration, R. E. Ansorge *et al.*, “Charged Particle Multiplicity Distributions at 200-GeV and 900-GeV Center-Of-Mass Energy,” *Z. Phys.* **C43** (1989) 357.
- [19] Z. Koba, H. B. Nielsen, and P. Olesen, “Scaling of multiplicity distributions in high-energy hadron collisions,” *Nucl. Phys.* **B40** (1972) 317–334.
- [20] **UA5** Collaboration, R. E. Ansorge *et al.*, “Charged Particle Correlations in $\bar{P}P$ Collisions at c.m. Energies of 200-GeV, 546-GeV and 900-GeV,” *Z. Phys.* **C37** (1988) 191–213.
- [21] **UA1** Collaboration, G. Arnison *et al.*, “Transverse Momentum Spectra for Charged Particles at the CERN Proton anti-Proton Collider,” *Phys. Lett.* **B118** (1982) 167–172.
- [22] **UA1** Collaboration, C. Albajar *et al.*, “A Study of the General Characteristics of $p\bar{p}$ Collisions at $\sqrt{s} = 0.2\text{-TeV}$ to 0.9-TeV ,” *Nucl. Phys.* **B335** (1990) 261–287.
- [23] **Ames-Bologna-CERN-Dortmund-Heidelberg-Warsaw** Collaboration, A. Breakstone *et al.*, “Multiplicity Dependence of Transverse Momentum Spectra at ISR Energies,” *Phys. Lett.* **B132** (1983) 463–466.
- [24] **UA1** Collaboration, F. Ceradini, “STUDY OF MINIMUM BIAS TRIGGER EVENTS AT $s^{*(1/2)} = 0.2\text{-TeV}$ TO 0.9-TeV WITH MAGNETIC AND CALORIMETRIC ANALYSIS AT THE CERN PROTON - ANTI-PROTON COLLIDER,” *Conf. Proc.* **C850718** (1985) 363.
- [25] **UA1** Collaboration, C. Albajar *et al.*, “Production of Low Transverse Energy Clusters in anti-p p Collisions at $s^{*(1/2)} = 0.2\text{-TeV}$ to 0.9-TeV and their Interpretation in Terms of QCD Jets,” *Nucl. Phys.* **B309** (1988) 405–425.

- [26] **UA1** Collaboration, G. Arnison *et al.*, “Hadronic Jet Production at the CERN Proton - anti-Proton Collider,” *Phys. Lett.* **B132** (1983) 214.
- [27] **Axial Field Spectrometer** Collaboration, T. Akesson *et al.*, “Double Parton Scattering in pp Collisions at $\sqrt{s} = 63\text{-GeV}$,” *Z. Phys.* **C34** (1987) 163.
- [28] P. V. Landshoff and J. C. Polkinghorne, “Calorimeter Triggers for Hard Collisions,” *Phys. Rev.* **D18** (1978) 3344.
- [29] C. Goebel, F. Halzen, and D. M. Scott, “Double Drell-Yan Annihilations in Hadron Collisions: Novel Tests of the Constituent Picture,” *Phys. Rev.* **D22** (1980) 2789.
- [30] N. Paver and D. Treleani, “Multi - Quark Scattering and Large p_T Jet Production in Hadronic Collisions,” *Nuovo Cim.* **A70** (1982) 215.
- [31] N. Paver and D. Treleani, “Multiple Parton Interactions and Multi - Jet Events at Collider and Tevatron Energies,” *Phys. Lett.* **B146** (1984) 252–256.
- [32] B. Humpert, “ARE THERE MULTI - QUARK INTERACTIONS?,” *Phys. Lett.* **B131** (1983) 461–467.
- [33] B. Humpert and R. Odorico, “Multiparton Scattering and QCD Radiation as Sources of Four Jet Events,” *Phys. Lett.* **B154** (1985) 211.
- [34] N. Paver and D. Treleani, “MULTIPLE PARTON PROCESSES IN THE TeV REGION,” *Z. Phys.* **C28** (1985) 187.
- [35] D. Treleani and G. Calucci. this book.
- [36] V. N. Gribov, “A REGGEON DIAGRAM TECHNIQUE,” *Sov. Phys. JETP* **26** (1968) 414–422. [*Zh. Eksp. Teor. Fiz.*53,654(1967)].
- [37] V. A. Abramovsky, V. N. Gribov, and O. V. Kancheli, “Character of Inclusive Spectra and Fluctuations Produced in Inelastic Processes by Multi - Pomeron Exchange,” *Yad. Fiz.* **18** (1973) 595–616. [*Sov. J. Nucl. Phys.*18,308(1974)].
- [38] G. Veneziano, “Regge Intercepts and Unitarity in Planar Dual Models,” *Nucl. Phys.* **B74** (1974) 365–377.
- [39] G. F. Chew and C. Rosenzweig, “Dual Topological Unitarization: An Ordered Approach to Hadron Theory,” *Phys. Rept.* **41** (1978) 263–327.
- [40] A. Capella, U. Sukhatme, C.-I. Tan, and J. Tran Thanh Van, “Jets in Small $p(T)$ Hadronic Collisions, Universality of Quark Fragmentation, and Rising Rapidity Plateaus,” *Phys. Lett.* **B81** (1979) 68–74.
- [41] H. Minakata, “Universal Quark - Jet Fragmentation in Soft Hadronic Reactions,” *Phys. Rev.* **D20** (1979) 1656.
- [42] G. Cohen-Tannoudji, A. El Hassouni, J. Kalinowski, O. Napoly, and R. B. Peschanski, “PARTONS AT LOW $P(T)$,” *Phys. Rev.* **D21** (1980) 2699.

- [43] K. Fialkowski and A. Kotanski, “Hadron Multiplicity Distributions in a Dual Model,” *Phys. Lett.* **B107** (1981) 132.
- [44] P. Aurenche and F. W. Bopp, “Rapidity Spectra in Proton Proton and Proton - Anti-proton Scattering Up to 540-GeV in a Dual Parton Model,” *Phys. Lett.* **B114** (1982) 363–368.
- [45] A. Capella and J. Tran Thanh Van, “Multiplicity Distributions Up to $s^{**}(1/2) = 540\text{-GeV}$ in the Dual Parton Model,” *Phys. Lett.* **B114** (1982) 450–456.
- [46] A. B. Kaidalov, “The Quark-Gluon Structure of the Pomeron and the Rise of Inclusive Spectra at High-Energies,” *Phys. Lett.* **B116** (1982) 459–463.
- [47] A. B. Kaidalov and K. A. Ter-Martirosian, “Pomeron as Quark-Gluon Strings and Multiple Hadron Production at SPS Collider Energies,” *Phys. Lett.* **B117** (1982) 247–251.
- [48] T. K. Gaisser and F. Halzen, “Soft Hard Scattering in the TeV Range,” *Phys. Rev. Lett.* **54** (1985) 1754.
- [49] G. Pancheri and Y. Srivastava, “Jets in Minimum Bias Physics,” *Conf. Proc.* **C850313** (1985) 28. [Phys. Lett.B159,69(1985)].
- [50] A. D. Martin and C. J. Maxwell, “Isolation of Hard Scattering Effects in Minimum Bias Data,” *Phys. Lett.* **B172** (1986) 248.
- [51] F. E. Paige and S. D. Protopopescu, “ISAJET 5.02: A MONTE CARLO EVENT GENERATOR FOR p p and anti-p p INTERACTIONS,” *Conf. Proc.* **C850809** (1985) 41.
- [52] R. Odorico, “Cojets: A Monte Carlo Program Simulating QCD in Hadronic Production of Jets and Heavy Flavors with Inclusion of Initial QCD Bremsstrahlung,” *Comput. Phys. Commun.* **32** (1984) 139.
- [53] R. D. Field, “High-energy Multi - Jets at the CERN $\bar{p}p$ Collider and the SSC,” *Nucl. Phys.* **B264** (1986) 687–720.
- [54] P. Aurenche, F. W. Bopp, and J. Ranft, “PARTICLE PRODUCTION IN HADRON HADRON COLLISIONS AT COLLIDER ENERGIES IN AN EXCLUSIVE MULTISTRING FRAGMENTATION MODEL,” *Z.Phys.* **C23** (1984) 67–76.
- [55] **UA5** Collaboration, G. J. Alner *et al.*, “The UA5 High-Energy anti-p p Simulation Program,” *Nucl. Phys.* **B291** (1987) 445–502.
- [56] **NNPDF** Collaboration, R. D. Ball, V. Bertone, S. Carrazza, L. Del Debbio, S. Forte, A. Guffanti, N. P. Hartland, and J. Rojo, “Parton distributions with QED corrections,” *Nucl. Phys.* **B877** (2013) 290–320, [arXiv:1308.0598](https://arxiv.org/abs/1308.0598) [hep-ph].
- [57] V. V. Sudakov, “Vertex parts at very high-energies in quantum electrodynamics,” *Sov. Phys. JETP* **3** (1956) 65–71. [Zh. Eksp. Teor. Fiz.30,87(1956)].

- [58] A. Buckley *et al.*, “General-purpose event generators for LHC physics,” *Phys. Rept.* **504** (2011) 145–233, [arXiv:1101.2599 \[hep-ph\]](#).
- [59] T. Sjöstrand, S. Mrenna, and P. Z. Skands, “PYTHIA 6.4 Physics and Manual,” *JHEP* **05** (2006) 026, [arXiv:hep-ph/0603175 \[hep-ph\]](#).
- [60] R. K. Ellis and J. C. Sexton, “QCD Radiative Corrections to Parton Parton Scattering,” *Nucl. Phys.* **B269** (1986) 445–484.
- [61] T. Sjöstrand and P. Z. Skands, “Multiple interactions and the structure of beam remnants,” *JHEP* **03** (2004) 053, [hep-ph/0402078](#).
- [62] L. V. Gribov, E. M. Levin, and M. G. Ryskin, “Semihard Processes in QCD,” *Phys. Rept.* **100** (1983) 1–150.
- [63] A. H. Mueller and J.-w. Qiu, “Gluon Recombination and Shadowing at Small Values of x ,” *Nucl. Phys.* **B268** (1986) 427–452.
- [64] R. J. Glauber, “High-Energy Collision Theory,” in *Lectures in Theoretical Physics*, W. E. Brittin and L. G. Dunham, eds., vol. I, pp. 315 – 414. Interscience, New York, 1959.
- [65] T. T. Chou and C.-N. Yang, “Model of Elastic High-Energy Scattering,” *Phys. Rev.* **170** (1968) 1591–1596.
- [66] C. Bourrely, J. Soffer, and T. T. Wu, “Impact Picture Expectations for Very High-Energy Elastic pp and $p\bar{p}$ Scattering,” *Nucl. Phys.* **B247** (1984) 15–28.
- [67] P. L’Heureux, B. Margolis, and P. Valin, “QUARK - GLUON MODEL FOR DIFFRACTION AT HIGH-ENERGIES,” *Phys. Rev.* **D32** (1985) 1681–1691.
- [68] G. ’t Hooft, “A Planar Diagram Theory for Strong Interactions,” *Nucl. Phys.* **B72** (1974) 461.
- [69] B. Andersson, G. Gustafson, and B. Söderberg, “A Probability Measure on Parton and String States,” *Nucl. Phys.* **B264** (1986) 29. [[145\(1985\)](#)].
- [70] H. Fritzsche, “Producing Heavy Quark Flavors in Hadronic Collisions: A Test of Quantum Chromodynamics,” *Phys. Lett.* **67B** (1977) 217–221.
- [71] A. Ali, J. G. Körner, G. Kramer, and J. Willrodt, “Nonleptonic Weak Decays of Bottom Mesons,” *Z. Phys.* **C1** (1979) 269.
- [72] H. Fritzsche, “How to Discover the B Mesons,” *Phys. Lett.* **B86** (1979) 343–346.
- [73] T. Alexopoulos *et al.*, “The role of double parton collisions in soft hadron interactions,” *Phys. Lett.* **B435** (1998) 453–457.
- [74] **E735** Collaboration, T. Alexopoulos *et al.*, “Charged particle multiplicity correlations in $p\bar{p}$ collisions at $\sqrt{s} = 0.3\text{-TeV}$ to 1.8-TeV ,” *Phys. Lett.* **B353** (1995) 155–160.

- [75] **E735** Collaboration, T. Alexopoulos *et al.*, “Multiplicity dependence of transverse momentum spectra of centrally produced hadrons in anti-p p collisions at 0.3-TeV, 0.54-TeV, 0.9-TeV, and 1.8-TeV center-of-mass energy,” *Phys. Lett.* **B336** (1994) 599–604.
- [76] **CDF** Collaboration, D. Acosta *et al.*, “Soft and hard interactions in $p\bar{p}$ collisions at $\sqrt{s} = 1800\text{-GeV}$ and 630-GeV ,” *Phys. Rev.* **D65** (2002) 072005.
- [77] **CDF** Collaboration, F. Abe *et al.*, “Double parton scattering in $\bar{p}p$ collisions at $\sqrt{s} = 1.8\text{TeV}$,” *Phys. Rev.* **D56** (1997) 3811–3832.
- [78] **CDF** Collaboration, T. Affolder *et al.*, “Charged jet evolution and the underlying event in $p\bar{p}$ collisions at 1.8 TeV,” *Phys. Rev.* **D65** (2002) 092002.
- [79] **CDF** Collaboration, R. D. Field, “The Underlying event in hard scattering processes,” *eConf* **C010630** (2001) P501, [arXiv:hep-ph/0201192](#) [hep-ph].
- [80] **CDF** Collaboration, D. Acosta *et al.*, “The underlying event in hard interactions at the Tevatron $\bar{p}p$ collider,” *Phys. Rev.* **D70** (2004) 072002, [arXiv:hep-ex/0404004](#) [hep-ex].
- [81] D. Kar, *Using Drell-Yan to probe the underlying event in Run II at Collider Detector at Fermilab (CDF)*. PhD thesis, Florida U., 2008.
- [82] **CDF** Collaboration, R. Field and R. C. Group, “PYTHIA tune A, HERWIG, and JIMMY in Run 2 at CDF,” [arXiv:hep-ph/0510198](#) [hep-ph].
- [83] **CDF** Collaboration, R. D. Field, “Studying the underlying event at CDF,” *Conf. Proc.* **C060726** (2006) 581–584. [581(2006)].
- [84] G. A. Schuler and T. Sjöstrand, “Hadronic diffractive cross-sections and the rise of the total cross-section,” *Phys. Rev.* **D49** (1994) 2257–2267.
- [85] A. Donnachie and P. V. Landshoff, “Total cross-sections,” *Phys. Lett.* **B296** (1992) 227–232, [arXiv:hep-ph/9209205](#) [hep-ph].
- [86] J. Dischler and T. Sjöstrand, “A Toy model of color screening in the proton,” *Eur. Phys. J. direct* **3** no. 1, (2001) 2, [arXiv:hep-ph/0011282](#) [hep-ph].
- [87] M. Glück, E. Reya, and A. Vogt, “Dynamical parton distributions of the proton and small x physics,” *Z. Phys.* **C67** (1995) 433–448.
- [88] G. A. Schuler and T. Sjöstrand, “Towards a complete description of high-energy photoproduction,” *Nucl. Phys.* **B407** (1993) 539–605.
- [89] G. A. Schuler and T. Sjöstrand, “A Scenario for high-energy gamma gamma interactions,” *Z. Phys.* **C73** (1997) 677–688, [arXiv:hep-ph/9605240](#) [hep-ph].
- [90] M. Ciafaloni, “Coherence Effects in Initial Jets at Small q^{*2} / s ,” *Nucl. Phys.* **B296** (1988) 49–74.

- [91] S. Catani, F. Fiorani, and G. Marchesini, “Small x Behavior of Initial State Radiation in Perturbative QCD,” *Nucl. Phys.* **B336** (1990) 18–85.
- [92] V. N. Gribov and L. N. Lipatov, “Deep inelastic $e p$ scattering in perturbation theory,” *Sov. J. Nucl. Phys.* **15** (1972) 438–450. [*Yad. Fiz.*15,781(1972)].
- [93] G. Altarelli and G. Parisi, “Asymptotic Freedom in Parton Language,” *Nucl. Phys.* **B126** (1977) 298–318.
- [94] Y. L. Dokshitzer, “Calculation of the Structure Functions for Deep Inelastic Scattering and $e^+ e^-$ Annihilation by Perturbation Theory in Quantum Chromodynamics,” *Sov. Phys. JETP* **46** (1977) 641–653. [*Zh. Eksp. Teor. Fiz.*73,1216(1977)].
- [95] E. A. Kuraev, L. N. Lipatov, and V. S. Fadin, “The Pomeron Singularity in Nonabelian Gauge Theories,” *Sov. Phys. JETP* **45** (1977) 199–204. [*Zh. Eksp. Teor. Fiz.*72,377(1977)].
- [96] I. I. Balitsky and L. N. Lipatov, “The Pomeron Singularity in Quantum Chromodynamics,” *Sov. J. Nucl. Phys.* **28** (1978) 822–829.
- [97] B. Andersson, G. Gustafson, and J. Samuelsson, “The Linked dipole chain model for DIS,” *Nucl. Phys.* **B467** (1996) 443–478.
- [98] G. Marchesini and B. R. Webber, “Monte Carlo Simulation of General Hard Processes with Coherent QCD Radiation,” *Nucl. Phys.* **B310** (1988) 461–526.
- [99] J. M. Butterworth, J. R. Forshaw, and M. H. Seymour, “Multiparton interactions in photoproduction at HERA,” *Z. Phys.* **C72** (1996) 637–646, [arXiv:hep-ph/9601371](#) [[hep-ph](#)].
- [100] I. Borozan and M. H. Seymour, “An Eikonal model for multiparticle production in hadron hadron interactions,” *JHEP* **09** (2002) 015, [arXiv:hep-ph/0207283](#) [[hep-ph](#)].
- [101] J. Bellm *et al.*, “Herwig 7.0/Herwig++ 3.0 release note,” *Eur. Phys. J.* **C76** no. 4, (2016) 196, [arXiv:1512.01178](#) [[hep-ph](#)].
- [102] M. Bähr, S. Gieseke, and M. H. Seymour, “Simulation of multiple partonic interactions in Herwig++,” *JHEP* **07** (2008) 076, [arXiv:0803.3633](#) [[hep-ph](#)].
- [103] S. Gieseke, F. Loshaj, and P. Kirchgaesser, “Soft and diffractive scattering with the cluster model in Herwig,” *Eur. Phys. J.* **C77** no. 3, (2017) 156, [arXiv:1612.04701](#) [[hep-ph](#)].
- [104] T. Gleisberg, S. Hoeche, F. Krauss, M. Schonherr, S. Schumann, F. Siegert, and J. Winter, “Event generation with SHERPA 1.1,” *JHEP* **02** (2009) 007, [arXiv:0811.4622](#) [[hep-ph](#)].
- [105] A. D. Martin, H. Hoeth, V. A. Khoze, F. Krauss, M. G. Ryskin, and K. Zapp, “Diffractive Physics,” *PoS QNP2012* (2012) 017, [arXiv:1206.2124](#) [[hep-ph](#)].

- [106] P. Aurenche, F. W. Bopp, A. Capella, J. Kwiecinski, M. Maire, J. Ranft, and J. Tran Thanh Van, “Multiparticle production in a two component dual parton model,” *Phys. Rev.* **D45** (1992) 92–105.
- [107] P. Aurenche, F. W. Bopp, R. Engel, D. Pertermann, J. Ranft, *et al.*, “DTUJET-93: Sampling inelastic proton proton and anti-proton - proton collisions according to the two component dual parton model,” *Comput.Phys.Commun.* **83** (1994) 107–123, [arXiv:hep-ph/9402351](#) [hep-ph].
- [108] R. Engel, “Photoproduction within the two component dual parton model. 1. Amplitudes and cross-sections,” *Z. Phys.* **C66** (1995) 203–214.
- [109] R. Engel and J. Ranft, “Hadronic photon-photon interactions at high-energies,” *Phys. Rev.* **D54** (1996) 4244–4262, [arXiv:hep-ph/9509373](#).
- [110] F. W. Bopp, J. Ranft, R. Engel, and S. Roesler, “Antiparticle to Particle Production Ratios in Hadron- Hadron and d-Au Collisions in the DPMJET-III Monte Carlo,” *Phys. Rev.* **C77** (2008) 014904, [arXiv:hep-ph/0505035](#).
- [111] R. S. Fletcher, T. K. Gaisser, P. Lipari, and T. Stanev, “SIBYLL: An Event generator for simulation of high-energy cosmic ray cascades,” *Phys. Rev.* **D50** (1994) 5710–5731.
- [112] E.-J. Ahn, R. Engel, T. K. Gaisser, P. Lipari, and T. Stanev, “Cosmic ray interaction event generator SIBYLL 2.1,” *Phys. Rev.* **D80** (2009) 094003, [arXiv:0906.4113](#) [hep-ph].
- [113] K. Werner, F.-M. Liu, and T. Pierog, “Parton ladder splitting and the rapidity dependence of transverse momentum spectra in deuteron gold collisions at RHIC,” *Phys. Rev.* **C74** (2006) 044902, [arXiv:hep-ph/0506232](#).
- [114] T. Pierog, I. Karpenko, J. M. Katzy, E. Yatsenko, and K. Werner, “EPOS LHC: Test of collective hadronization with data measured at the CERN Large Hadron Collider,” *Phys. Rev.* **C92** no. 3, (2015) 034906, [arXiv:1306.0121](#) [hep-ph].
- [115] K. Werner, B. Guiot, I. Karpenko, A. G. Knospe, C. Markert, T. Pierog, and G. Sophys. this book.
- [116] S. Ostapchenko, “Nonlinear screening effects in high energy hadronic interactions,” *Phys. Rev.* **D74** no. 1, (2006) 014026, [arXiv:hep-ph/0505259](#) [hep-ph].
- [117] S. Ostapchenko, “Monte Carlo treatment of hadronic interactions in enhanced Pomeron scheme: I. QGSJET-II model,” *Phys. Rev.* **D83** (2011) 014018, [arXiv:1010.1869](#) [hep-ph].
- [118] T. Sjöstrand and P. Z. Skands, “Baryon number violation and string topologies,” *Nucl. Phys.* **B659** (2003) 243, [arXiv:hep-ph/0212264](#) [hep-ph].
- [119] T. Sjöstrand and P. Z. Skands, “Transverse-momentum-ordered showers and interleaved multiple interactions,” *Eur. Phys. J.* **C39** (2005) 129–154, [hep-ph/0408302](#).

- [120] T. Sjöstrand, S. Mrenna, and P. Z. Skands, “A Brief Introduction to PYTHIA 8.1,” *Comput. Phys. Commun.* **178** (2008) 852–867, [arXiv:0710.3820 \[hep-ph\]](#).
- [121] R. Corke and T. Sjöstrand, “Interleaved Parton Showers and Tuning Prospects,” *JHEP* **03** (2011) 032, [arXiv:1011.1759 \[hep-ph\]](#).
- [122] R. Corke and T. Sjöstrand, “Multiparton interactions and rescattering,” *JHEP* **01** (2009) 035, [arXiv:0911.1909 \[hep-ph\]](#).
- [123] B. Blok, Yu. Dokshitzer, L. Frankfurt, and M. Strikman, “pQCD physics of multiparton interactions,” *Eur. Phys. J.* **C72** (2012) 1963, [arXiv:1106.5533 \[hep-ph\]](#).
- [124] M. Diehl, D. Ostermeier, and A. Schafer, “Elements of a theory for multiparton interactions in QCD,” *JHEP* **03** (2012) 089, [arXiv:1111.0910 \[hep-ph\]](#).
- [125] J. R. Gaunt, “Single Perturbative Splitting Diagrams in Double Parton Scattering,” *JHEP* **01** (2013) 042, [arXiv:1207.0480 \[hep-ph\]](#).
- [126] M. Diehl, J. R. Gaunt, and K. Schönwald, “Double hard scattering without double counting,” [arXiv:1702.06486 \[hep-ph\]](#).
- [127] M. Diehl and J. R. Gaunt. this book.
- [128] K. Konishi, A. Ukawa, and G. Veneziano, “Jet Calculus: A Simple Algorithm for Resolving QCD Jets,” *Nucl. Phys.* **B157** (1979) 45–107.
- [129] R. Kirschner, “Generalized Lipatov-Altarelli-Parisi Equations and Jet Calculus Rules,” *Phys. Lett.* **B84** (1979) 266–270.
- [130] V. P. Shelest, A. M. Snigirev, and G. M. Zinovev, “The Multiparton Distribution Equations in QCD,” *Phys. Lett.* **B113** (1982) 325.
- [131] A. M. Snigirev, “Double parton distributions in the leading logarithm approximation of perturbative QCD,” *Phys. Rev.* **D68** (2003) 114012, [arXiv:hep-ph/0304172 \[hep-ph\]](#).
- [132] V. L. Korotkikh and A. M. Snigirev, “Double parton correlations versus factorized distributions,” *Phys. Lett.* **B594** (2004) 171–176, [arXiv:hep-ph/0404155 \[hep-ph\]](#).
- [133] J. W. Cronin *et al.*, “Production of Hadrons with Large Transverse Momentum at 200-GeV, 300-GeV, and 400-GeV,” *Phys. Rev.* **D11** (1975) 3105.
- [134] E. Avsar, G. Gustafson, and L. Lönnblad, “Small-x dipole evolution beyond the large-N(c) limit,” *JHEP* **01** (2007) 012, [arXiv:hep-ph/0610157](#).
- [135] C. Bierlich, G. Gustafson, L. Lönnblad, and A. Tarasov, “Effects of Overlapping Strings in pp Collisions,” *JHEP* **03** (2015) 148, [arXiv:1412.6259 \[hep-ph\]](#).
- [136] G. Gustafson and L. Lönnblad. this book.

- [137] L. Frankfurt, M. Strikman, and C. Weiss, “Small-x physics: From HERA to LHC and beyond,” *Ann. Rev. Nucl. Part. Sci.* **55** (2005) 403–465, [arXiv:hep-ph/0507286](#).
- [138] M. Strikman. this book.
- [139] R. Corke and T. Sjöstrand, “Multiparton Interactions with an x-dependent Proton Size,” *JHEP* **05** (2011) 009, [arXiv:1101.5953 \[hep-ph\]](#).
- [140] **ATLAS** Collaboration, “Summary of ATLAS Pythia 8 tunes,”.
- [141] G. Ingelman and P. E. Schlein, “Jet Structure in High Mass Diffractive Scattering,” *Phys. Lett.* **B152** (1985) 256–260.
- [142] **UA8** Collaboration, R. Bonino *et al.*, “Evidence for Transverse Jets in High Mass Diffraction,” *Phys. Lett.* **B211** (1988) 239.
- [143] P. Bruni and G. Ingelman, “Diffractive W and Z production at p anti-p colliders and the pomeron parton content,” *Phys. Lett.* **B311** (1993) 317–323.
- [144] S. Navin, “Diffraction in Pythia,” [arXiv:1005.3894 \[hep-ph\]](#).
- [145] R. Ciesielski and K. Goulianos, “MBR Monte Carlo Simulation in PYTHIA8,” *PoS ICHEP2012* (2013) 301, [arXiv:1205.1446 \[hep-ph\]](#).
- [146] Y. L. Dokshitzer, V. A. Khoze, and T. Sjöstrand, “Rapidity gaps in Higgs production,” *Phys. Lett.* **B274** (1992) 116–121.
- [147] J. D. Bjorken, “Rapidity gaps and jets as a new physics signature in very high-energy hadron hadron collisions,” *Phys. Rev.* **D47** (1993) 101–113.
- [148] **CDF** Collaboration, T. Affolder *et al.*, “Diffractive dijets with a leading antiproton in $\bar{p}p$ collisions at $\sqrt{s} = 1800$ GeV,” *Phys. Rev. Lett.* **84** (2000) 5043–5048.
- [149] C. O. Rasmussen and T. Sjöstrand, “Hard Diffraction with Dynamic Gap Survival,” *JHEP* **02** (2016) 142, [arXiv:1512.05525 \[hep-ph\]](#).
- [150] J. R. Christiansen and T. Sjöstrand, “Color reconnection at future $e^+ e^-$ colliders,” *Eur. Phys. J.* **C75** no. 9, (2015) 441, [arXiv:1506.09085 \[hep-ph\]](#).
- [151] T. Sjöstrand, “Colour Reconnections from LEP to Future Colliders,” in *Proceedings, Parton Radiation and Fragmentation from LHC to FCC-ee: CERN, Geneva, Switzerland, November 22-23, 2016*, pp. 144–148. 2017.
- [152] T. Sjöstrand and V. A. Khoze, “On Color rearrangement in hadronic W^+W^- events,” *Z. Phys.* **C62** (1994) 281–310, [arXiv:hep-ph/9310242](#).
- [153] **ALEPH, DELPHI, L3, OPAL, LEP Electroweak** Collaboration, S. Schael *et al.*, “Electroweak Measurements in Electron-Positron Collisions at W-Boson-Pair Energies at LEP,” *Phys.Rept.* **532** (2013) 119–244, [arXiv:1302.3415 \[hep-ex\]](#).

- [154] T. Sjöstrand, S. Ask, J. R. Christiansen, R. Corke, N. Desai, P. Ilten, S. Mrenna, S. Prestel, C. O. Rasmussen, and P. Z. Skands, “An Introduction to PYTHIA 8.2,” *Comput. Phys. Commun.* **191** (2015) 159–177, [arXiv:1410.3012 \[hep-ph\]](#).
- [155] J. R. Christiansen and P. Z. Skands, “String Formation Beyond Leading Colour,” *JHEP* **08** (2015) 003, [arXiv:1505.01681 \[hep-ph\]](#).
- [156] P. Skands and D. Wicke, “Non-perturbative QCD effects and the top mass at the Tevatron,” *Eur. Phys. J.* **C52** (2007) 133–140, [arXiv:hep-ph/0703081](#).
- [157] S. Argyropoulos and T. Sjöstrand, “Effects of color reconnection on $t\bar{t}$ final states at the LHC,” *JHEP* **1411** (2014) 043, [arXiv:1407.6653 \[hep-ph\]](#).
- [158] A. Buckley and H. Schulz. this book.
- [159] P. Z. Skands, “Tuning Monte Carlo Generators: The Perugia Tunes,” *Phys. Rev.* **D82** (2010) 074018, [arXiv:1005.3457 \[hep-ph\]](#).
- [160] H. Schulz and P. Z. Skands, “Energy Scaling of Minimum-Bias Tunes,” *Eur. Phys. J.* **C71** (2011) 1644, [arXiv:1103.3649 \[hep-ph\]](#).
- [161] P. Skands, S. Carrazza, and J. Rojo, “Tuning PYTHIA 8.1: the Monash 2013 Tune,” *Eur. Phys. J.* **C74** no. 8, (2014) 3024, [arXiv:1404.5630 \[hep-ph\]](#).
- [162] C. M. Buttar, D. Clements, I. Dawson, and A. Moraes, “Simulations of minimum bias events and the underlying event, MC tuning and predictions for the LHC,” *Acta Phys. Polon.* **B35** (2004) 433–441.
- [163] **ATLAS** Collaboration, “ATLAS Monte Carlo tunes for MC09,”.
- [164] **ATLAS** Collaboration, “ATLAS tunes of PYTHIA 6 and Pythia 8 for MC11,”.
- [165] **ATLAS** Collaboration, “ATLAS Pythia 8 tunes to 7 TeV data,”.
- [166] **ATLAS** Collaboration, G. Aad *et al.*, “Measurement of the Z/γ^* boson transverse momentum distribution in pp collisions at $\sqrt{s} = 7$ TeV with the ATLAS detector,” *JHEP* **09** (2014) 145, [arXiv:1406.3660 \[hep-ex\]](#).
- [167] **CMS** Collaboration, V. Khachatryan *et al.*, “Event generator tunes obtained from underlying event and multiparton scattering measurements,” *Eur. Phys. J.* **C76** no. 3, (2016) 155, [arXiv:1512.00815 \[hep-ex\]](#).
- [168] A. Buckley, H. Hoeth, H. Lacker, H. Schulz, and J. E. von Seggern, “Systematic event generator tuning for the LHC,” *Eur. Phys. J.* **C65** (2010) 331–357, [arXiv:0907.2973 \[hep-ph\]](#).
- [169] A. Buckley, J. Butterworth, L. Lonnblad, D. Grellscheid, H. Hoeth, J. Monk, H. Schulz, and F. Siegert, “Rivet user manual,” *Comput. Phys. Commun.* **184** (2013) 2803–2819, [arXiv:1003.0694 \[hep-ph\]](#).

- [170] A. Karneyeu, L. Mijovic, S. Prestel, and P. Z. Skands, “MCPLLOTS: a particle physics resource based on volunteer computing,” *Eur. Phys. J.* **C74** (2014) 2714, [arXiv:1306.3436 \[hep-ph\]](#).
- [171] N. Fischer and T. Sjöstrand, “Thermodynamical String Fragmentation,” *JHEP* **01** (2017) 140, [arXiv:1610.09818 \[hep-ph\]](#).
- [172] **ALICE** Collaboration, J. Adam *et al.*, “Enhanced production of multi-strange hadrons in high-multiplicity proton-proton collisions,” *Nature Phys.* **13** (2017) 535–539, [arXiv:1606.07424 \[nucl-ex\]](#).
- [173] **ALICE** Collaboration, B. B. Abelev *et al.*, “Production of $\Sigma(1385)^\pm$ and $\Xi(1530)^0$ in proton-proton collisions at $\sqrt{s} = 7$ TeV,” *Eur. Phys. J.* **C75** no. 1, (2015) 1, [arXiv:1406.3206 \[nucl-ex\]](#).
- [174] **STAR** Collaboration, B. I. Abelev *et al.*, “Strange particle production in p+p collisions at $s^{*(1/2)} = 200$ -GeV,” *Phys. Rev.* **C75** (2007) 064901, [arXiv:nucl-ex/0607033 \[nucl-ex\]](#).
- [175] **ATLAS** Collaboration, G. Aad *et al.*, “Charged-particle multiplicities in pp interactions measured with the ATLAS detector at the LHC,” *New J. Phys.* **13** (2011) 053033, [arXiv:1012.5104 \[hep-ex\]](#).
- [176] **CMS** Collaboration, S. Chatrchyan *et al.*, “Charged particle transverse momentum spectra in *pp* collisions at $\sqrt{s} = 0.9$ and 7 TeV,” *JHEP* **08** (2011) 086, [arXiv:1104.3547 \[hep-ex\]](#).
- [177] **ALICE** Collaboration, J. Adam *et al.*, “Pseudorapidity and transverse-momentum distributions of charged particles in proton-proton collisions at $\sqrt{s} = 13$ TeV,” *Phys. Lett.* **B753** (2016) 319–329, [arXiv:1509.08734 \[nucl-ex\]](#).
- [178] **ALICE** Collaboration, J. Adam *et al.*, “Measurement of pion, kaon and proton production in proton-proton collisions at $\sqrt{s} = 7$ TeV,” *Eur. Phys. J.* **C75** no. 5, (2015) 226, [arXiv:1504.00024 \[nucl-ex\]](#).
- [179] **CMS** Collaboration, V. Khachatryan *et al.*, “Strange Particle Production in *pp* Collisions at $\sqrt{s} = 0.9$ and 7 TeV,” *JHEP* **05** (2011) 064, [arXiv:1102.4282 \[hep-ex\]](#).
- [180] **CMS** Collaboration, V. Khachatryan *et al.*, “Observation of Long-Range Near-Side Angular Correlations in Proton-Proton Collisions at the LHC,” *JHEP* **09** (2010) 091, [arXiv:1009.4122 \[hep-ex\]](#).
- [181] **ATLAS** Collaboration, G. Aad *et al.*, “Observation of Long-Range Elliptic Azimuthal Anisotropies in $\sqrt{s} = 13$ and 2.76 TeV *pp* Collisions with the ATLAS Detector,” *Phys. Rev. Lett.* **116** no. 17, (2016) 172301, [arXiv:1509.04776 \[hep-ex\]](#).
- [182] **CMS** Collaboration, V. Khachatryan *et al.*, “Evidence for collectivity in pp collisions at the LHC,” *Phys. Lett.* **B765** (2017) 193–220, [arXiv:1606.06198 \[nucl-ex\]](#).

- [183] C. Bierlich, G. Gustafson, and L. Lönnblad, “A shoving model for collectivity in hadronic collisions,” [arXiv:1612.05132](#) [hep-ph].
- [184] K. J. Eskola, K. Kajantie, and J. Lindfors, “Quark and Gluon Production in High-Energy Nucleus-Nucleus Collisions,” *Nucl. Phys.* **B323** (1989) 37–52.
- [185] M. H. Seymour and A. Siodmok, “Extracting $\sigma_{\text{effective}}$ from the LHCb double-charm measurement,” [arXiv:1308.6749](#) [hep-ph].
- [186] A. Bialas and R. B. Peschanski, “Moments of Rapidity Distributions as a Measure of Short Range Fluctuations in High-Energy Collisions,” *Nucl. Phys.* **B273** (1986) 703–718.
- [187] A. Bialas and R. B. Peschanski, “Intermittency in Multiparticle Production at High-Energy,” *Nucl. Phys.* **B308** (1988) 857–867.
- [188] **UA1** Collaboration, C. Albajar *et al.*, “Intermittency studies in anti-p p collisions at $s^{*(1/2)} = 630\text{-GeV}$,” *Nucl. Phys.* **B345** (1990) 1–21.
- [189] E. A. De Wolf, I. M. Dremin, and W. Kittel, “Scaling laws for density correlations and fluctuations in multiparticle dynamics,” *Phys. Rept.* **270** (1996) 1–141, [arXiv:hep-ph/9508325](#) [hep-ph].